https://doi.org/10.5194/bg-2023-30
Preprint. Discussion started: 2 March 2023

Biogeosciences Discussions

A Modeling Approach to Investigate Drivers, Variability and Uncertainties in O_2 Fluxes and the O_2:CO_2 Exchange Ratios in a Temperate Forest

Yuan Yan[1], Anne Klosterhalfen[1], Fernando Moyano[1], Matthias Cuntz[2], Andrew C. Manning[3], Alexander Knohl[1,4]

[1] Bioclimatology, University of Goettingen, 37077 Goettingen, Germany
[2] Université de Lorraine, AgroParisTech, INRAE, UMR Silva, 54000 Nancy, France
[3] Centre for Ocean and Atmospheric Sciences, School of Environmental Sciences, University of East Anglia, Norwich, NR4 7TJ, United Kingdom
[4] Centre of Biodiversity and Sustainable Land Use (CBL), University of Goettingen, 37073 Goettingen, Germany

Correspondence to: Yuan Yan (yuanyantwincities@gmail.com)

Abstract. The O_2:CO_2 exchange ratio (ER) between terrestrial ecosystems and the atmosphere is a key parameter for partitioning global ocean and land carbon fluxes. The long-term terrestrial ER is considered to be close to 1.10 moles of O_2 consumed per mole of CO_2 produced. Due to the technical challenge in measuring directly the ER of entire terrestrial ecosystems (ER_{eco}), little is known about the variations in ER at the hourly and seasonal scales as well as how different components contribute to ER_{eco}. In this modeling study, we explore the variability and drivers of ER_{eco} and evaluate the hypothetical uncertainty in determining ecosystem O_2 fluxes based on current instrument precision. We adapted the one-dimensional, multi-layer atmosphere-biosphere gas exchange model, CANVEG, to simulate hourly ER_{eco} from modeled O_2 and CO_2 fluxes in a temperate beech forest in Germany.

We found that the annual mean ER_{eco} ranged from 1.06 to 1.12 mol mol^{-1} within the five years' study period. Hourly ER_{eco} showed strong variations over diel and seasonal cycles and within the vertical canopy profile. Determination of ER from O_2 and CO_2 mole fractions in air above and within the canopy (ER_{conc}) varied between 1.115 and 1.15 mol mol^{-1}. CANVEG simulations also indicated that ecosystem O_2 fluxes could be derived using the flux-gradient method in combination with measurements of vertical scalar gradients and CO_2, sensible heat or latent heat fluxes obtained with the eddy covariance technique. Owing to measurement uncertainties, however, the uncertainty in estimated O_2 fluxes derived with the flux-gradient approach could be as high as 15 μmol m^{-2} s^{-1}, which represented the 90% quantile of the uncertainty in hourly data with a high-accuracy instrument. We also demonstrated that O_2 fluxes can be used to partition net CO_2 exchange fluxes into their component fluxes of photosynthesis and respiration, if ER_{eco} is known. The uncertainty of the partitioned gross assimilation ranged from 1.43 to 4.88 μmol m^{-2} s^{-1} assuming a measurement uncertainty of 0.1 or 2.5 μmol m^{-2} s^{-1} for net ecosystem CO_2 exchange and from 0.1 to 15 μmol m^{-2} s^{-1} for net ecosystem O_2 exchange, respectively. Our analysis suggests that O_2 measurements at ecosystem scale have the potential for partitioning net CO_2 fluxes into their component fluxes, but further improvement in instrument precision is needed.

https://doi.org/10.5194/bg-2023-30
Preprint. Discussion started: 2 March 2023

1 Introduction

Fluxes of O_2 and CO_2 between the terrestrial biosphere and atmosphere are inversely linked in photosynthesis, which assimilates CO_2 and releases O_2, and in respiration, which consumes O_2 and releases CO_2 (Keeling and Manning, 2014; Severinghaus, 1995). The relationship between these opposing fluxes can be described with the so-called O_2:CO_2 exchange ratio (ER, see Table A1 in the Appendix for an overview of all abbreviations and variable names used here), which should be considered on various temporal and spatial scales – ranging from hourly to decadal temporal and from leaf to global spatial scales. Since the relationship between O_2 and CO_2 fluxes between the atmosphere and different carbon reservoirs (terrestrial biosphere, oceans and fossil fuels) differ on regional and global scales, these different ERs can be applied as parameters in global models in conjunction with observations of atmospheric O_2 and CO_2 abundances to quantify the global sinks of CO_2 in the ocean and in the biosphere (Battle et al., 2000; Ishidoya et al., 2012; Keeling and Manning, 2014; Keeling and Shertz, 1992; Tohjima et al., 2019). The global ER for the land biota is commonly set to 1.1 moles of O_2 consumed per mole of CO_2 produced (or vice versa) (Severinghaus, 1995) by assuming that this value, derived from elemental abundance data, is a representative long-term average for all land biota (Keeling and Manning, 2014; Manning and Keeling, 2006). An ER of 1.05 mol mol^{-1} was determined by Randerson et al. (2006) based on observed chemical compositions of plant parts for quantification of the global carbon sink. Measurements using the oxidative ratio of organic material provided a more recent terrestrial ER estimate of 1.04 ± 0.03 mol mol^{-1} (Worrall et al., 2013). Using an ER of 1.05 mol mol^{-1} instead of 1.1 mol mol^{-1} in carbon budget models will attribute 0.05 Pg C yr^{-1} more to the global land carbon sink and an equivalent amount less to the ocean sink (Keeling and Manning, 2014), indicating that the ER should be well constrained when parameterized in global ocean and land carbon cycle models.

On ecosystem-scale, a mole fraction-based and a flux-based O_2:CO_2 ratio can be considered (Ishidoya et al., 2013; Seibt et al., 2004). The former is defined as the fluctuations in the mole fraction of O_2 per mole fraction of CO_2 in the atmosphere (ER_{conc}). Thus, ER_{conc} is usually derived from the slopes of linear regressions between observed atmospheric O_2 and CO_2 mole fractions (Battle et al., 2019; Ishidoya et al., 2013; Seibt et al., 2004). Battle et al. (2019) observed an average ER_{conc} = 1.08 ± 0.007 mol mol^{-1} in a mixed deciduous forest over a six years' period with temporal variations on a 6-hour basis between 0.85 and 1.15 mol mol^{-1}. Measurements of canopy air O_2 and CO_2 mole fractions at two different forest sites yielded ER_{conc} estimations between 1.01 and 1.03 mol mol^{-1} averaged over 24-hour periods and between 1.14 and 1.19 mol mol^{-1} during daytime only (Seibt et al., 2004). Ishidoya et al. (2013) obtained differing ER_{conc} at two heights within a cool temperate deciduous forest, reflecting variations of ER_{conc} with canopy height. Furthermore, they observed different ER_{conc} during daytime (0.87 mol mol^{-1}) and nighttime (1.03 mol mol^{-1}) in summer, indicating a significant variation of ER_{conc} over the diel period (Ishidoya et al., 2013). Faassen et al. (2022) found the much higher ER_{conc} over 24 hours (2.05 ± 0.03 mol mol^{-1}) than for daytime (1.1 ± 0.12 mol mol^{-1}) and nighttime (1.22 ± 0.02 mol mol^{-1}) due to the variation of the boundary layer height during the measurement period.

https://doi.org/10.5194/bg-2023-30
Preprint. Discussion started: 2 March 2023

The flux-based O_2:CO_2 ratio is defined as the O_2 flux per CO_2 flux between an ecosystem and the atmosphere (ER_{eco}). Flux estimates can be described as the net turbulent exchange or the overall net exchange (turbulent plus storage flux), where we focus on the latter in this study. Only very few studies have attempted to quantify ER_{eco} because measuring O_2 fluxes at ecosystem scale is still a major challenge. Since O_2 and CO_2 are strongly anti-correlated in the processes of photosynthesis and respiration, changes in both scalars are very similar in absolute numbers, typically in the order of a few ppm. However, the relative changes in O_2 are much smaller than in CO_2 owing to the much higher atmospheric abundance (around 210,000 ppm for O_2 and around 400 ppm for CO_2), making O_2 measurements at sufficient precision and accuracy technically challenging. Thus, studies resorted to, for instance, the flux-gradient method, chamber measurements and modeling approaches (see below). Ishidoya et al. (2015) determined a daily mean net turbulent ER = 0.86 mol mol^{-1} based on O_2 and CO_2 gradient measurements. Faassen et al. (2022) reported daytime and nighttime ER_{eco} as 0.92 ± 0.17 and 1.03 ± 0.05 mol mol^{-1}, respectively. In general, ER_{eco} depends on the elemental composition and reduction state of organic material, and on the temporal variation and spatial distribution of sinks and sources of ecosystem flux components (Seibt et al., 2004). According to Battle et al. (2019), the dynamics and interrelations of the various sinks and sources within the ecosystem, each with their own ER_{eco}, result in the mixed signal ER_{conc}.

Current micrometeorological approaches to measure gas exchange between ecosystems and the atmosphere include eddy covariance, flux-gradient and eddy accumulation methods, which could all theoretically be used to determine ecosystem O_2 fluxes. The applicability of the eddy covariance technique for O_2 flux estimation, however, requires high precision at a high measurement frequency (10-20 Hz). Except for a homemade, non-commercial vacuum ultraviolet (VUV) absorption analyzer (Stephens et al., 2003) no suitable instrument exists so far.

With the flux-gradient method, O_2 fluxes can be inferred from an O_2 gradient above a canopy and an eddy diffusivity (K), which can be derived based on additional CO_2, sensible or latent heat flux measurements (Baldocchi et al., 1988). This method assumes that heat and mass are transported in a similar manner between two adjacent levels above the canopy (Baldocchi et al., 1988). The method's applicability is again particularly challenging for O_2 estimates owing to the typically large measurement uncertainty in relation to the small O_2 gradient. One approach to increase the measurement-to-noise ratio is to move the lower inlet of the gradient measurement closer to or even inside the canopy. This approach, however, violates the assumption of the flux-gradient method owing to infrequent but predominantly large eddies within the canopy, counter-gradient fluxes and possible non-differentiable gradients (Raupach, 1989; Wilson, 1989). The flux-gradient method has already been used for O_2 flux estimation above a cool temperate forest (Ishidoya et al., 2015), an urban canopy (Ishidoya et al., 2020) and a boreal forest (Faassen et al., 2022). The theoretical limits of the flux-gradient method for O_2 fluxes given current instrument precision and accuracy are, however, not yet fully explored.

Chamber level gas exchange measurements provide an alternative approach to measure the ER of individual components such as leaf, stem and soil, which could be scaled up to ecosystem level. Chamber measurements in a German temperate forest showed an average ER of leaf net assimilation (ER_{An}; net assimilation defined as carboxylation minus photorespiration and dark respiration) between 1.08 ± 0.16 mol mol^{-1} and 1.19 ± 0.12 mol mol^{-1}, and an ER of soil respiration (ER_{soil}) of 0.94 ± 0.04

https://doi.org/10.5194/bg-2023-30
Preprint. Discussion started: 2 March 2023

mol mol^{-1} (Seibt et al., 2004). In a cool temperate deciduous forest in Japan, gas exchange chamber measurements indicated an ER_{An} = 1.02 ± 0.03 mol mol^{-1} and ER_{soil} = 1.11 ± 0.01 mol mol^{-1} (Ishidoya et al., 2013). Hilman et al. (2019) measured an average ER of stem respiration (ER_{stem}) between 0.97 and 1.95 mol mol^{-1} for tropical, temperate and Mediterranean trees with a closed-flow chamber system with two continuous flow analyzers.

The ER variability in assimilation and respiration fluxes found in the studies mentioned above provides a potential approach to partition net CO_2 fluxes into their components following similar approaches based on stable isotopes in CO_2 (Knohl and Buchmann, 2005; Ogee et al., 2004; Wehr and Saleska, 2015; Zobitz et al., 2007). Using simultaneous measurements of net ecosystem O_2 and CO_2 fluxes and considering the ER for the photosynthetic and respiratory processes in a canopy and at the soil surface, two mass balance equations can be written for O_2 and CO_2 (see Eq. (1) below). Hourly or half-hourly ER would be needed to agree with the typical time step of flux estimates derived with the eddy covariance technique, which is the standard method of measuring gas exchange between land surfaces and the atmosphere (Baldocchi et al., 2001; Goulden et al., 1996). Theoretically, such an O_2-based partitioning method only works for periods when the ER of gross assimilation (ER_A) and gross ecosystem respiration (ER_R) differ, because a second independent mass balance equation is needed to yield CO_2 fluxes of assimilation (F_A) and respiration (F_R). According to Ogee et al. (2004), the difference in ER has to be large enough to obtain a reasonable accuracy in the partitioned net CO_2 fluxes. Consequently, an analysis of temporal dynamics in ER_A and ER_R is necessary in order to evaluate the possibility of applying O_2 observations in a CO_2 flux partitioning approach.

The contribution of flux components to the temporal and spatial variability on overall ecosystem O_2 fluxes can also be explored by modeling approaches. For example, net turbulent ER was simulated with a simple one-box model with daily time steps, by assuming that O_2 and CO_2 mole fractions are spatially constant and temporally variable within the canopy (Ishidoya et al., 2015; Seibt et al., 2004). These simulations indicated that variations in net turbulent ER are not only influenced by leaf and soil fluxes, but also by turbulence inside and outside the canopy (Seibt et al., 2004). To explore the drivers of ER variations at ecosystem scale, more precise turbulence effects need to be considered. However, simple one-box models assume uniform and well-mixed air columns throughout the canopy, so that modeled ER lacks variations for different layers within the canopy.

Multi-layer atmosphere-biosphere models such as CANVEG (Baldocchi, 1997; Baldocchi and Wilson, 2001) differ from one-box models in that they are designed to represent the temporal and (vertical) spatial scale of an eddy covariance tower. Therefore, they are a good simulator to test and examine new types of observations (Oikawa et al., 2017). CANVEG includes within-canopy transport of CO_2, water vapor and energy (Baldocchi, 1997; Baldocchi and Wilson, 2001), so that if it were adapted to O_2 processes, one could evaluate the accuracy of different flux measurement techniques such as eddy covariance or flux-gradient approaches. Published ER values of gross and/or net assimilation, stem respiration and soil respiration can be employed as parameters to derive component-specific O_2 fluxes from existing modeled CO_2 fluxes. Thus, concurrent O_2 and CO_2 fluxes, and ER can be simulated for multiple canopy layers and for the whole ecosystem, with which we can analyze the main drivers of modeled ER values, their diel and seasonal variability, and vertical variations. In addition, concurrently simulated mole fraction profiles – a function of turbulent dispersion and the strength and location of scalar sources and sinks – enable us to test the precision of the flux-gradient method for O_2 flux estimation while choosing various measurement heights

https://doi.org/10.5194/bg-2023-30
Preprint. Discussion started: 2 March 2023

inside and above the canopy. Furthermore, the performance of an O_2-based source partitioning method can be evaluated based on model simulations.

Based on these considerations, we defined the following study objectives: (1) to implement atmosphere-biosphere O_2:CO_2 exchange ratios for various ecosystem components in the multi-layer CANVEG model; (2) to explore temporal and spatial variations in O_2:CO_2 exchange ratios as well as the underlying main drivers at ecosystem scale; (3) to evaluate the potential precision of the flux-gradient approach to obtain O_2 fluxes; and (4) to evaluate the feasibility of O_2 flux measurements for CO_2 flux partitioning.

2 Methods

2.1 Site description

The meteorological and plant-specific ecophysiological measurements used in the model simulation were derived from the Leinefelde FLUXNET tower site (DE-Lnf, https://doi.org/10.18140/FLX/1440150) located in central Germany (51°19′42”N, 10°22′04”E, 450 m a.s.l.; (Anthoni et al., 2004)). The vegetation at the site is an even-aged managed beech stand (*Fagus sylvatica* L.) with an age of approximately 130 years (Tamrakar et al., 2018). The mean annual temperature was 8.3 ± 0.7 °C and the average cumulative annual precipitation was 600 ± 150 mm between 2002 and 2016 (Braden-Behrens et al., 2019). The canopy height (ht) is 37.5 m and maximum effective leaf area index (LAI) was approximately 4.8 m^2 m^{-2} in 2015 (Braden-Behrens et al., 2017).

Meteorological variables including air temperature, air humidity, direct and diffuse global radiation, photosynthetic photon flux density, wind velocity, air pressure, vapor pressure deficit, precipitation, atmospheric CO_2 mole fraction ($CO_{2\ atm}$), soil temperature and soil moisture, as well as fluxes of net ecosystem CO_2 exchange (F_{CO_2}), sensible heat (H), and latent heat (LE) obtained with the eddy covariance technique are continuously measured at 44 m above the forest canopy (Anthoni et al., 2004). The meteorological variables were used as input data for our model simulations, while the flux estimates were storage-term corrected and then used for model calibration and validation (see below). In this paper, upward fluxes (release to the atmosphere) are presented as positive quantities and downward fluxes (uptake by the ecosystem) as negative quantities. Thus, O_2 fluxes always have opposite signs to their corresponding CO_2 fluxes, which is in line with micrometeorological conventions.

2.2 Model description and model set-up

We used the one-dimensional, multi-layer atmosphere-biosphere gas exchange model, “CANVEG”, described by Baldocchi (1997) and Baldocchi and Wilson (2001). The model domain includes 120 model layers above the ground, in which the lower 40 above-ground layers cover the entire canopy, while the bottom layer represents the soil surface for the description of soil carbon and energy fluxes. The domain also includes 10 below-ground soil layers; however, this study did not consider processes within the soil column in detail. CANVEG uses hourly meteorological variables as drivers, as well as site-specific

https://doi.org/10.5194/bg-2023-30
Preprint. Discussion started: 2 March 2023

parameters (see Table 1) to simulate biosphere-atmosphere water vapor, CO_2 and energy fluxes within and above the forest canopy.

The carbon, water and energy modules in CANVEG have been validated for various environmental conditions and forest types (Baldocchi, 1997; Baldocchi et al., 2002; Baldocchi et al., 1999). Moreover, CANVEG has previously been applied to an unmanaged beech-dominated forest site only 30 km away from the site of this study (Knohl and Baldocchi, 2008), and has recently been used to simulate the isotopic composition of carbon assimilates at Leinefelde (Braden-Behrens et al., 2019). We translated the original C code (Baldocchi, 1997) to Fortran 90, which was then used for further implementations.

Atmospheric O_2 mole fraction ($O_{2\ atm}$) as input for the model was deduced from a fixed O_2:CO_2 mole ratio of -1.15 mol mol^{-1} (R^2 = 0.99) and continuous CO_2 mole fraction measurements at the site (Table 1). The fixed O_2:CO_2 mole ratio was derived from measurements at the University of Göttingen from November 2017 to January 2018 using a high-precision O_2 measurement system developed by Dr. Penelope Pickers (University of East Anglia, UK) and very similar to the system described in Pickers et al. (2017).

Some model parameters regarding leaf photosynthesis, stomatal conductance and soil respiration were fitted to the actual site conditions via the Markov Chain Monte Carlo (MCMC) method (Van Oijen et al., 2005). Eddy covariance measurements of hourly F_{CO_2}, H and LE, and the estimated ecosystem respiration (F_R) in 2012 and 2013 were used to calibrate the model parameters (

Table 1). The years 2014-2016 were used for model validation. The leaf phenology parameters, including day of year (DOY) for the start of leaf growth, end of leaf growth, start of leaf fall and end of leaf fall ($leaf_{out}$, $leaf_{full}$, $leaf_{fall}$, and $leaf_{fall\_complete}$) were derived from daily camera images in 2015 above the canopy. LAI within the annual course was simulated based on these four parameters: The DOY before $leaf_{out}$ and after $leaf_{fall\_complete}$ were defined as winter when LAI = zero and between $leaf_{full}$ and $leaf_{fall}$ as summer when LAI = 4.8 m^2 m^{-2}. During spring ($leaf_{out}$ < DOY < $leaf_{full}$) and during autumn ($leaf_{fall}$ < DOY < $leaf_{fall\_complete}$) LAI increased or decreased linearly and accordingly. The maximum LAI of 4.8 m^2 m^{-2} as well as the LAI fraction (f_{LAI}) at five different heights in the canopy were measured using a LI-2000 plant canopy analyzer (LI-COR Biosciences GmbH, Germany) in 2015 (Braden-Behrens et al., 2017). The vertical LAI profile was assumed to follow a beta-distribution, which was fitted to the observed f_{LAI} (Table 1). This relationship between LAI and height (z) allocates leaves mainly in the upper canopy (z/ht ≥ 0.45) with almost no leaves in the bottom canopy (Fig. 1a). The wood area index (WAI) consisted of the branches (80% of total WAI) and the stems (20% of total WAI). The branches were situated in the upper canopy (z/ht ≥ 0.45) following the same distribution algorithm of LAI, while in the lower canopy (z/ht < 0.45), the fraction of stem WAI per layer to total stem area was deduced from the fraction of stem diameter per layer to the diameter at breast height (f_{DBH}) as a function of height (z): $f_{DBH} = 102 - 2.6z + 0.08z^2 - 0.0023z^3$ (Schober, 1952). This set-up of the forest canopy including leaf phenology and the vertical LAI and WAI profiles was used for all years of the model run. All site-specific parameters used in this study are listed in Table 1.

For the simulation of net ecosystem O_2 fluxes (F_{O_2}), values of ER had to be chosen: the input parameter of ER_A was set to 1.00 mol mol^{-1} (Table 1), by assuming that photosynthesis produces glucose ($C_6H_{12}O_6$), resulting in equal O_2 and CO_2 fluxes. The

https://doi.org/10.5194/bg-2023-30
Preprint. Discussion started: 2 March 2023

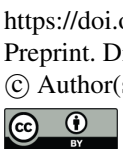

ER of canopy respiration was attributed to the ER of leaf dark respiration (ER_{rd}) and stem respiration (ER_{stem}). ER_{stem} was fixed to 1.04 mol mol^{-1} (Randerson et al., 2006), while the ER_{rd} was set to increase with leaf temperature (T_{leaf}; Fig. 1b) according to Tcherkez et al. (2003). ER_{soil} was set to 1.1 mol mol^{-1} (Randerson et al., 2006; Severinghaus, 1995).

To validate the model, we used eddy covariance measurements of F_{CO_2}, H and LE from 2014 to 2016. And to quantify the model performance, we calculated the slope, intercept, and the coefficient of determination (R^2) of a linear regression between modeled and observed F_{CO_2}, H and LE, as well as the root mean squared error (RMSE).

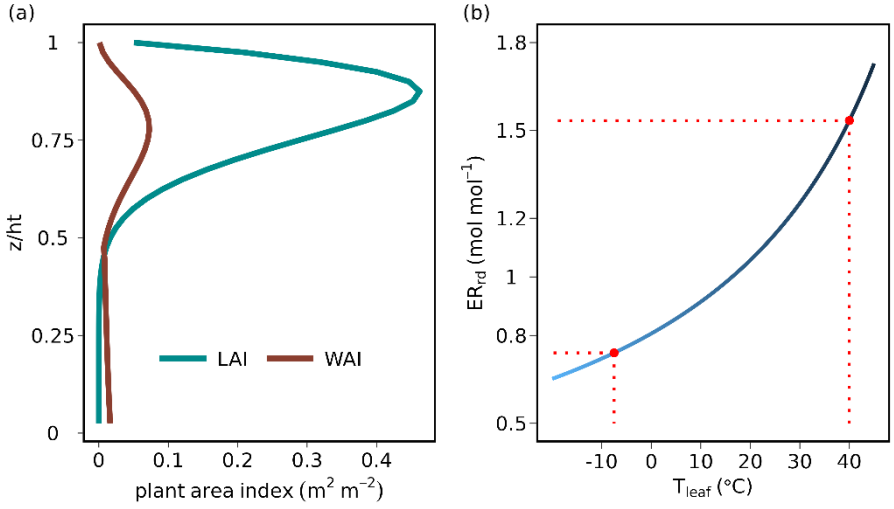

Figure 1. (a) Distribution of vertical leaf and wood area indices (LAI and WAI in m^2 m^{-2} per canopy layer) used in the CANVEG model, derived from measurements at the Leinefelde study site (Braden-Behrens et al., 2017). The y-axis is the ratio of the height in the canopy (z) to the top of the canopy (ht). (b) O_2:CO_2 exchange ratio of leaf dark respiration (ER_{rd} in mol mol^{-1}) as a function of leaf temperature (T_{leaf} in °C) after Tcherkez et al. (2003). The red dashed lines indicate the range of T_{leaf} and corresponding ER_{rd} in this study.

Table 1. Model parameters adjusted to the study site Leinefelde, Germany.

Parameter name	Details	Value
k_{ball}	slope of Ball-Berry model after Collatz et al. (1991)	10.4 *
b	intercept of Ball-Berry model after Collatz et al. (1991)	0.0014 µmol m^{-2} s^{-1} *
V_{cmax25}	maximum carboxylation at 25 °C	59.6 µmol m^{-2} s^{-1} *
R_{d25}	leaf dark respiration at 25 °C	0.0149 · V_{cmax25} *
J_{max25}	maximum electron transport rate at 25 °C	2.24 · V_{cmax25} *
θ_J	curvature parameter of light response curve	0.882 *
α	fraction of the photosystem II activity	0.284 *

https://doi.org/10.5194/bg-2023-30
Preprint. Discussion started: 2 March 2023

r_1, r_2	coefficients for exponential relationship between soil temperature and soil respiration	0.827, 0.075 *
$leaf_{out}$	DOY for the start of leaf growth	110
$leaf_{full}$	DOY for the end of leaf growth	130
$leaf_{fall}$	DOY for the start of leaf fall	282
$leaf_{fall\_complete}$	DOY for the end of leaf fall	320
LAI	leaf area index	4.8 m^2 m^{-2}
f_{LAI}	fraction of LAI per layer	0, 0.04, 0.66, 0.2, 0.1 at 7.5, 17, 28, 32.5 and 37.5 m
$O_{2\ atm}$	atmospheric O_2 mole fraction	$O_{2\ atm}$ = -1.15 $CO_{2\ atm}$ + 209749.5 (ppm)
ht	canopy height	37.5 m
ER_A	O_2:CO_2 exchange ratio of gross assimilation	1.00 mol mol^{-1}
ER_{rd}	O_2:CO_2 exchange ratio of leaf dark respiration depending on leaf temperature (°C)	$ER_{rd} = \frac{1}{-0.0147\ T_{leaf} + 1.24}$ (mol mol^{-1}) (Tcherkez et al., 2003)
ER_{stem}	O_2:CO_2 exchange ratio of stem respiration	1.04 mol mol^{-1} (Randerson et al., 2006)
ER_{soil}	O_2:CO_2 exchange ratio of soil respiration	1.10 mol mol^{-1} (Severinghaus, 1995)

* Parameters were calibrated with eddy covariance measurements of hourly F_{CO_2}, F_R, H and LE in 2012 and 2013 via the Markov Chain Monte Carlo (MCMC) method.

2.3. Model simulations of flux- and mole fraction-based exchange ratios

In CANVEG, CO_2 fluxes are simulated for the leaf, stem and soil components. The O_2 fluxes of each component are estimated by scaling each corresponding CO_2 flux by its ER. Respiratory CO_2 fluxes are defined to be positive, while assimilation CO_2 fluxes are negative. O_2 fluxes always have the opposite sign from the corresponding CO_2 fluxes, which would result in negative ER values. However, we have defined all ER parameters to be positive by including the factor (-1) in all relevant equations (see below), to be consistent with most published literature concerning O_2:CO_2 exchange ratios (Ishidoya et al., 2013; Seibt et al., 2004). Another way of considering this is that the ERs are the ratios of moles of O_2 consumed per mole of CO_2 produced (or moles of O_2 produced per mole of CO_2 consumed).

The O_2 and CO_2 ecosystem fluxes are the balance of the simulated fluxes of gross assimilation (F_A, carboxylation minus photorespiration) and gross ecosystem respiration (F_R). The latter consists of leaf dark respiration (F_{rd}), stem respiration (F_{stem}) and soil respiration (F_{soil}, consisting of 50% respiration by heterotrophs and 50% by autotrophs):

$$\begin{cases} F_{CO_2} = F_A + F_{rd} + F_{stem} + F_{soil} = F_A + F_R \\ F_{O_2} = -F_A\,ER_A - F_{rd}\,ER_{rd} - F_{stem}\,ER_{stem} - F_{soil}\,ER_{soil} = -F_A\,ER_A - F_R\,ER_R \end{cases} \quad (1)$$

https://doi.org/10.5194/bg-2023-30
Preprint. Discussion started: 2 March 2023

where ER_A, ER_{rd}, ER_{stem} and ER_{soil} are given as model parameters (see Section 2.2.). The simulated F_{O_2} and F_{CO_2} include the storage fluxes associated with concentration changes of O_2 and CO_2 in the canopy air space, because they were inferred by integrating fluxes for all canopy layers.

For the model simulations, ER of the entire ecosystem, of the net assimilation at leaf level or of only respiratory processes can be obtained by considering the simulations of the corresponding flux components. The ER of the overall ecosystem (ER_{eco}) in hourly time steps was calculated as the ratio of the hourly F_{O_2} and F_{CO_2} (including storage terms) summed up over the entire canopy height, that is:

$$ER_{eco} = -\frac{F_{O_2}}{F_{CO_2}} \quad (2)$$

ER_{eco} for specific canopy heights (ER^z_{eco}) was derived as the slope of linear regressions fitted to O_2 and CO_2 fluxes of multiple simulated time steps for each canopy layer.

Furthermore, the simulated ER of net O_2 and CO_2 assimilation (ER_{An}) and of all respiratory fluxes (ER_R) were derived as:

$$ER_{A_n} = -\frac{-F_A\,ER_A - F_{rd}\,ER_{rd}}{F_A + F_{rd}} \quad (3)$$

$$ER_R = -\frac{-F_{rd}\,ER_{rd} - F_{stem}\,ER_{stem} - F_{soil}\,ER_{soil}}{F_{rd} + F_{stem} + F_{soil}} \quad (4)$$

The atmospheric O_2 mole fraction at each canopy layer was also computed by CANVEG, analogous to that done for CO_2 mole fraction (Baldocchi, 1997). CANVEG estimates atmospheric mole fraction per layer as a function of multi-layer gas flux diffusion determined by a Lagrangian dispersion matrix (Baldocchi, 1992) and the atmospheric background gas mole fraction. The mole fraction-based ER (ER_{conc}) and ER_{conc} in specific canopy heights (ER^z_{conc}) are defined as the ratio between the fluctuations in O_2 and CO_2 mole fractions, and both were calculated as the slopes of linear regressions fitted to hourly atmospheric O_2 versus CO_2 mole fractions for the growing seasons (the days of year with leaves for the canopy, between $leaf_{out}$ and $leaf_{fall\_complete}$) of all simulation years (Battle et al., 2019; Ishidoya et al., 2013; Seibt et al., 2004). Thus, we obtained ER^z_{eco} and ER^z_{conc} with the same approach by deriving the slopes of hourly data to allow a comparison.

2.4. Evaluation of the flux-gradient method to obtain O_2 fluxes

The CANVEG simulations of ecosystem O_2 fluxes and O_2 mole fraction gradients provided the opportunity to test the applicability of the flux-gradient approach to estimate F_{O_2}. We assumed the flux-gradient system can be installed both above the canopy and close to the forest floor. We especially aimed at testing the performance of the flux-gradient method based on current typical instrument performance for O_2 measurements. The turbulent O_2 ($\tilde{F_{O_2}}$), CO_2 ($\tilde{F_{CO_2}}$), sensible heat ($\tilde{H}$) and latent heat ($\tilde{LE}$) fluxes are related to vertical scalar gradients as follows (Meredith et al., 2014):

https://doi.org/10.5194/bg-2023-30
Preprint. Discussion started: 2 March 2023

$$\begin{cases} F_{\widetilde{O_2}} = -K_o \frac{\Delta o}{\Delta z} \rho_n \\ F_{\widetilde{CO_2}} = -K_c \frac{\Delta c}{\Delta z} \rho_n \\ H^{\sim} = -K_T \frac{\Delta T}{\Delta z} \rho_m c_p \\ LE^{\sim} = -K_v \frac{\Delta v}{\Delta z} \lambda \end{cases} \quad (5)$$

where Δz (m) is the vertical height difference, ΔT, Δv, Δc and Δo denote the vertical gradients of air temperature (K), water vapor (kg m^{-3}), CO_2 mole fraction (ppm) and O_2 mole fraction (ppm), respectively, ρ_n and ρ_m are the molar density (mol m^{-3}) and mass density of the air (kg m^{-3}), c_p is the specific heat capacity of air (J kg^{-1} K^{-1}), and λ is the latent heat of evaporation (J kg^{-1}). The superscript tilde in the flux nomenclatures denotes turbulent fluxes (without storage fluxes). K_o, K_c, K_T, and K_v (m^2 s^{-1}) are the eddy diffusivities of the relevant scalars. Assuming that heat and mass are transported in a similar way between two adjacent levels above the canopy and so assuming that $K_o=K_c=K_T=K_v$ (Baldocchi et al., 1988), O_2 fluxes can be estimated with each of the following equations:

$$\begin{cases} F_{\widetilde{O_2,c}} = F_{\widetilde{CO_2}} \frac{\Delta o}{\Delta c} \\ F_{\widetilde{O_2,T}} = H^{\sim} \frac{\Delta o \, \rho_n}{\Delta T \, \rho_m \, c_p} \\ F_{\widetilde{O_2,v}} = LE^{\sim} \frac{\Delta o \, \rho_n}{\Delta v \, \lambda} \end{cases} \quad (6)$$

From simulations of $F_{\widetilde{CO_2}}$, $H^{\sim}$ and $LE^{\sim}$ and vertical scalar profiles, we derived F_{O_2} from $F_{\widetilde{O_2}}$ plus the storage term based on the flux-gradient method and compared these to the directly modeled F_{O_2} (Eq. (1)). Here, the subscripts c, T and v denote which flux and scalar were used.

There are usually three sources of error in the flux-gradient method: (1) the uncertainty in the vertical gradient (that is, the gradient of O_2 mole fraction, Δo) resulting from the precision and accuracy of the measurement instruments, (2) the magnitude of the mole fraction difference (Δc, ΔT, or Δv) between two constant measurement heights, which is usually small when the measurement heights are too close to each other or when the atmosphere is well mixed, and (3) the measurement uncertainty in the turbulent fluxes ($F_{\widetilde{CO_2}}$, $H^{\sim}$, or $LE^{\sim}$), which we assumed to be zero, because we applied here only our simulated turbulent fluxes. So here, we quantified the extent of the first two sources of error, and defined conditions when the flux-gradient method could perform satisfactorily to obtain F_{O_2}. The effects of the first uncertainty were evaluated by adding a "measurement error" to Δo, where the error was assumed to be normally distributed with a mean of zero and a standard deviation of ±0.7 ppm, based on typical measurement uncertainty of the O_2 mole fraction instrument used to derive the fixed atmospheric O_2:CO_2 ratio (Pickers et al., 2017). Then the difference between the F_{O_2} derived via the flux-gradient method with and without the measurement error ($\sigma_{F_{O_2}}$) was evaluated.

https://doi.org/10.5194/bg-2023-30
Preprint. Discussion started: 2 March 2023

The second uncertainty due to the magnitude in the gradient as a function of Δz was analyzed by estimating F_{O_2} based on the flux-gradient between a top measurement height at two times the canopy height in our model set-up and each layer below, until the soil surface (z/ht = 0). The top measurement height was set to z/ht = 2 following customary recommendations for the setup of eddy covariance towers following Rebmann et al. (2018). We also included measurement heights inside the canopy, where the vertical profiles are mostly non-linear due to scalar sources and sinks, to illustrate the effect of violating the assumptions of the flux-gradient method. For comparison, the difference between the F_{O_2} estimations derived by the flux-gradient method ($\tilde{F}_{O_2,(c,T,v)}$, based on $\tilde{F}_{CO_2}$, $\tilde{H}$ or $\tilde{LE}$ and their respective vertical scalar profile) and by model simulations ($\tilde{F}_{O_2,CANVEG}$) was calculated:

$$diff_{F_{O_2,(c,T,v)}} = \tilde{F}_{O_2,(c,T,v)} - \tilde{F}_{O_2,CANVEG} \quad (7)$$

where $diff_{F_{O_2}}$ is the difference for the application between the top measurement height (z/ht = 2) and each layer below.

Finally, we also tested a three-heights flux-gradient method after the recent study of Faassen et al. (2022). They derived scalar concentrations at three heights (z/ht = 0.9, 3.7 and 6.9 with ht = 18 m), fitted a quadratic scalar-height relationship, and expressed the vertical gradient as the first derivative of z (see Eq. (10) and (11) by Faassen et al. (2022)). In our study, we selected the three heights at z/ht = 1.05, 1.45 and 2 with ht = 37.5 m, to be with all heights above the canopy.

2.5. Uncertainties in partitioning net ecosystem CO_2 fluxes based on O_2 fluxes

The net ecosystem CO_2 exchange (F_{CO_2}) consists of two different components: gross assimilation (F_A) and gross ecosystem respiration (F_R). Similar to the stable isotope flux partitioning approach (Bowling et al., 2001; Knohl and Buchmann, 2005; Ogee et al., 2004; Oikawa et al., 2017; Yakir and Wang, 1996), O_2 and CO_2 flux mass balance equations can be written as shown in Eq. (1), where F_{CO_2} is the observed ecosystem flux from eddy covariance measurements and F_{O_2} is obtained by multiplying F_{CO_2} by the modeled ER_{eco} in CANVEG following Eq. (2) (owing to the lack of actual F_{O_2} measurements). We treated these mass balance equations as a probabilistic process assuming terms on the right-hand side are uncertainty quantities with *a priori* values ($F_A^b, F_R^b, ER_A^b, ER_R^b$) and uncertainties ($\sigma_{F_A^b}, \sigma_{F_R^b}, \sigma_{ER_A^b}, \sigma_{ER_R^b}$). Fluxes and exchange ratios, i.e. F_A, F_R, ER_A and ER_R, can be then calculated that minimize the differences between the left-hand side observations and the right-hand side "model" under consideration of their uncertainties, leading to *a posteriori* quantities (F_A, F_R, ER_A, ER_R) with corresponding uncertainties ($\sigma_{F_A}, \sigma_{F_R}, \sigma_{ER_A}, \sigma_{ER_R}$). A cost function (J) was then written as a linear system with all the differences weighted by the corresponding *a priori* uncertainties:

$$J = \frac{1}{2}\left[\left(\frac{F_A+F_R-F_{CO_2}}{\sigma_{F_{CO_2}}}\right)^2 + \left(\frac{F_A\,ER_A+F_R\,ER_R-F_{O_2}}{\sigma_{F_{O_2}}}\right)^2 + \left(\frac{F_A-F_A^b}{\sigma_{F_A^b}}\right)^2 + \left(\frac{F_R-F_R^b}{\sigma_{F_R^b}}\right)^2 + \left(\frac{ER_A-ER_A^b}{\sigma_{ER_A^b}}\right)^2 + \left(\frac{ER_R-ER_R^b}{\sigma_{ER_R^b}}\right)^2\right] \quad (8)$$

https://doi.org/10.5194/bg-2023-30
Preprint. Discussion started: 2 March 2023

315

The last four terms allow a solution to be defined even with fewer equations than unknowns. The a posteriori values and uncertainties were returned at minimum J with predefined a priori values and uncertainties (Table 2). For the J function with multiple variables as in our case, the a posteriori means of any parameter, x, were found along the gradient of each variable where its Jacobian equaled zero ($\frac{\partial J}{\partial x} = 0$; (Tarantola, 2004)), while the corresponding a posteriori uncertainties were expressed

320 as the square root of the inverse Hessian at the minimum ($\frac{\partial^2 J}{\partial x^2}$; (Tarantola, 2004)):

$$\begin{bmatrix} \sigma_{F_A} \\ \sigma_{F_R} \\ \sigma_{ER_A} \\ \sigma_{ER_R} \end{bmatrix} = \sqrt{\begin{bmatrix} \frac{\partial^2 J}{\partial {F_A}^2} & \frac{\partial^2 J}{\partial F_A \partial F_R} & \frac{\partial^2 J}{\partial F_A \partial ER_A} & \frac{\partial^2 J}{\partial F_A \partial ER_R} \\ \frac{\partial^2 J}{\partial F_R \partial F_A} & \frac{\partial^2 J}{\partial {F_R}^2} & \frac{\partial^2 J}{\partial F_R \partial ER_A} & \frac{\partial^2 J}{\partial F_R \partial ER_R} \\ \frac{\partial^2 J}{\partial ER_A \partial F_A} & \frac{\partial^2 J}{\partial ER_A \partial F_R} & \frac{\partial^2 J}{\partial {ER_A}^2} & \frac{\partial^2 J}{\partial ER_A \partial ER_R} \\ \frac{\partial^2 J}{\partial ER_R \partial F_A} & \frac{\partial^2 J}{\partial ER_R \partial F_R} & \frac{\partial^2 J}{\partial ER_R \partial ER_A} & \frac{\partial^2 J}{\partial {ER_R}^2} \end{bmatrix}^{-1}} \quad (9)$$

By assuming no correlations among the variables, only the diagonal elements of the Hessian were used in a posteriori

325 uncertainties calculation.

We evaluated the a posteriori uncertainties on partitioned photosynthetic fluxes on a typical day during summer (4 July 2012) with assigned a priori uncertainties. The a priori uncertainty of gross assimilation ($\sigma_{F_A^b}$) was set to 10 μmol m^{-2} s^{-1} and of ecosystem respiration ($\sigma_{F_R^b}$) to 5 μmol m^{-2} s^{-1}, following Ogee et al. (2004) assuming less constraint on a posteriori results (Table 2). The uncertainty of the net CO_2 fluxes ($\sigma_{F_{CO_2}}$) was derived from Mann and Lenschow's model (Lenschow et al.,

330 1994) and calculated for our site to be 2.5 μmol m^{-2} s^{-1} (Braden-Behrens et al., 2019). We also examined if σ_{F_A} could be reduced if more accurate net CO_2 fluxes were measured ($\sigma_{F_{CO_2}}$ = 0.5 μmol m^{-2} s^{-1}).

The uncertainty of measured ecosystem O_2 fluxes ($\sigma_{F_{O_2}}$) is unknown to us. Consequently, we used the results from the flux-gradient method evaluation (section 2.4.). In order to clearly quantify the effect of $\sigma_{F_{O_2}}$ and σ_{ER_A} on flux partitioning precision, we defined a $\sigma_{F_{O_2}}$ series ranging from 0.1 to 15 μmol m^{-2} s^{-1}, representing 90% quantile of random Δo measurement

335 uncertainty (see section 2.4.), and a series of $\sigma_{ER_A^b}$ ranging from 0.001 to 0.1 mol mol^{-1}. $\sigma_{ER_R^b}$ was fixed to either 0.05 or 0.001 mol mol^{-1}.

Table 2. Assigned *a priori* values and uncertainties to build the cost function, J, for the uncertainty estimation of using O_2 fluxes to partition net CO_2 fluxes.

variables	*a priori* values	*a priori* uncertainties
F_A	-15 μmol m^{-2} s^{-1}	10 μmol m^{-2} s^{-1}

https://doi.org/10.5194/bg-2023-30
Preprint. Discussion started: 2 March 2023

F_R	5 µmol m^{-2} s^{-1}	5 µmol m^{-2} s^{-1}
ER_A	1 mol mol^{-1}	0.001 - 0.1 mol mol^{-1}
ER_R	1.1 mol mol^{-1}	0.05 or 0.001 mol mol^{-1}
F_{CO_2}	eddy covariance observations	2.5 or 0.1 µmol m^{-2} s^{-1}
F_{O_2}	CANVEG outputs	0.1 - 15 µmol m^{-2} s^{-1}

340

3 Results

3.1 Model performance

The model generally showed similar performance for F_{CO_2}, H and LE during both calibration and validation (Fig. 2), indicating robust model behavior as a multi-layer canopy flux simulator. The model validation for F_{CO_2} (R^2 = 0.82, slope = 1.016) was
345 generally better than for H (R^2 = 0.7, slope = 0.879) and LE (R^2 = 0.77, slope = 1.02) (Fig. 2b, 2d and 2f). The disagreement between modeled and measured F_{CO_2} indicates some uncertainties in the parameters for soil and stem respiration as well as phenology in the model equations. The similar scale but opposite sign of y-intercepts for H and LE calibration simulations (Fig. 2c and 2e) indicate underestimation in H and the same amount of overestimation in LE. The slopes deviating from one for H and LE could come from a non-closure of the energy balance in the eddy covariance observations.

350

https://doi.org/10.5194/bg-2023-30
Preprint. Discussion started: 2 March 2023

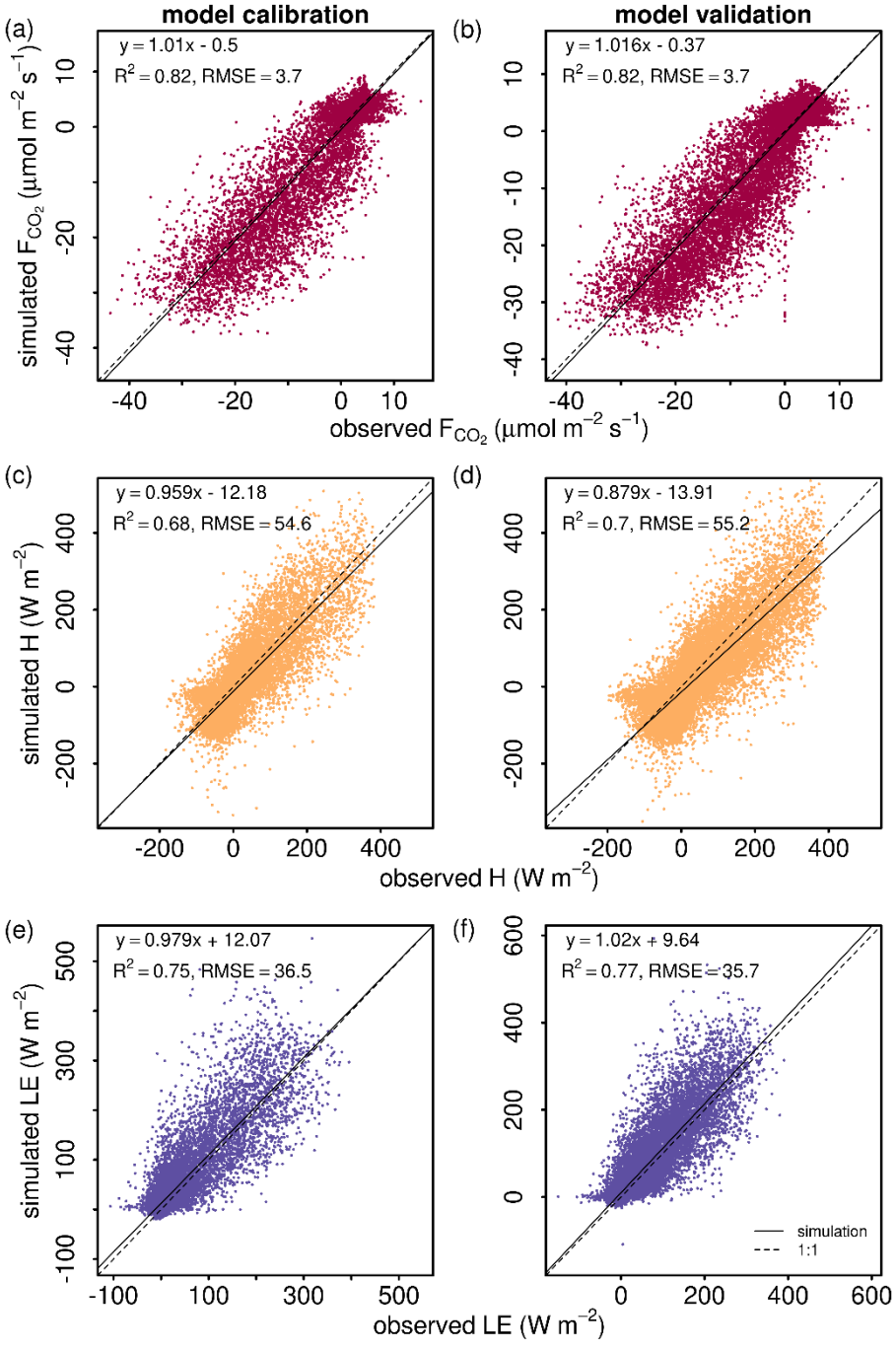

Figure 2. Comparison of (a), (b) net ecosystem CO_2 flux (F_{CO_2}), (c), (d) sensible (H), and (e), (f) latent (LE) heat flux from 2012 to 2016 between model simulations (y-axes) and eddy covariance observations (x-axes). The left column shows all hourly data points for the calibration period (2012-2013), and the right column shows all hourly data points for the validation period (2014-2016). The linear regression line function, coefficient of determination (R^2), and the root mean squared error (RMSE) are included in each panel. The dashed lines are the 1:1 lines.

https://doi.org/10.5194/bg-2023-30
Preprint. Discussion started: 2 March 2023

3.2 Temporal dynamics of O_2:CO_2 exchange ratios

The median of the hourly ecosystem O_2:CO_2 exchange ratio (ER_{eco}) throughout the simulation period (2012-2016) was 1.08 mol mol^{-1}, where the annual medians did not differ between years. The annual mean ER_{eco} ranged from 1.06 to 1.12 mol mol^{-1} across the five years. Hourly ER_{eco} also varied seasonally and within the diel course, as shown as an example for the year 2012 in Figure 3a. During the non-growing season, ER_{eco} were constrained between 1.04 and 1.10 mol mol^{-1}, representing a mixture of the prevailing stem and soil respiration processes. During the growing season, ER_{eco} was close to 1.00 mol mol^{-1} during daylight hours, due to the dominance of photosynthetic processes, and sometimes even smaller than 1.00 mol mol^{-1}, when daytime F_{O_2} was smaller than daytime F_{CO_2}. This can occur with ER_A = 1.00 mol mol^{-1}, and ER_{stem}, ER_{soil} and ER_{rd} > 1.00 mol mol^{-1} (following Eq. (1)) more O_2 was consumed than CO_2 released for the respiratory fluxes, and thus this decreased the magnitude of net F_{O_2}. During nighttime in the growing season, ER_{eco} was > 1.00 mol mol^{-1}, representing a mixture of stem, soil and leaf dark respiration. For transition periods (sunrise and sunset), with flux magnitudes close to zero, ER_{eco} values were very high, owing to very small F_{CO_2}. Because ER_{eco} is a ratio, values can get extremely large and approach infinity as F_{CO_2} approaches zero. However, since corresponding F_{O_2} values are also very low, these ER_{eco} values have very little effect on median and mean ER_{eco} of the overall ecosystem over a longer time period.

The median and mean of hourly O_2:CO_2 net assimilation ratio (ER_{An}) were 0.99 mol mol^{-1} and 0.96 mol mol^{-1}, respectively, for all growing seasons during the simulation period, and did not vary between years. Again, the seasonal and diel variations of ER_{An} in the year 2012 are shown in Figure 3b as an example. During nighttime, ER_{An} was equivalent to ER_{rd} and thus also dependent on T_{leaf} (Fig. 1b). With low T_{leaf} at the beginning or end of the growing season, ER_{An} was often smaller than 0.90 mol mol^{-1}. During daytime, when the magnitude of F_A was usually much larger than the magnitude of the opposing flux F_{rd}, ER_{An} was negatively correlated to T_{leaf}. Note that F_{rd} and ER_{rd} respond differently to T_{leaf}, that is, F_{rd} is a fraction of V_{cmax}, which has an optimal temperature at 27 °C (Table 1) while ER_{rd} is positively correlated with T_{leaf} (Fig. 1b). Consequently, during periods with high T_{leaf} and low irradiation, F_{rd} was small, but ER_{rd} was large and the magnitude of the O_2 flux of leaf respiration was larger than the magnitude of the CO_2 flux with $|-F_{rd} \cdot ER_{rd}| > |F_{rd}|$. Moreover, $|-F_A \cdot ER_A|$ and $|F_A|$ were small with ER_A = 1.00 mol mol^{-1}. It follows that under these conditions and given model implementation, ER_{An} describes the ratio of O_2 uptake and CO_2 uptake (both fluxes with the same sign), when more O_2 was consumed due to dark leaf respiration than released by assimilation ($|-F_{rd} \cdot ER_{rd}| > |-F_A \cdot ER_A|$). In addition, because values of F_A are below zero and values of F_{rd} are greater than zero, values of ER_{An} (Eq. (3)) lie mostly not between ER_A and ER_{rd}. Similar to ER_{eco}, high variations in ER_{An} were usually found during transition periods with low flux magnitudes.

https://doi.org/10.5194/bg-2023-30
Preprint. Discussion started: 2 March 2023

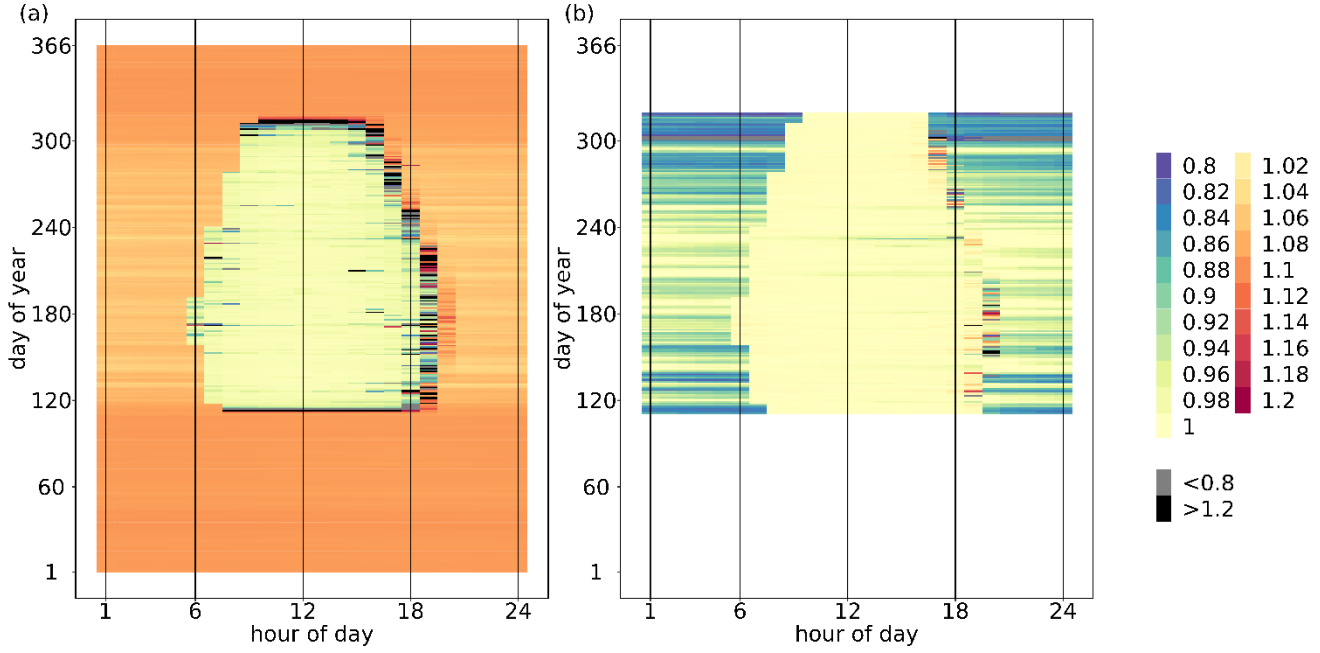

Figure 3. Temporal variations of (a) the exchange ratio of net ecosystem fluxes (ER_{eco}, mol mol^{-1}) and (b) the exchange ratio of net assimilation (ER_{An}, mol mol^{-1}) by hour of day and day of year in 2012. The exchange ratios were calculated as the ratio of the hourly F_{O_2} and F_{CO_2} (including storage terms) summed up over the entire canopy height. As a guide, 1st July is day 183.

3.3 Vertical profiles of O_2:CO_2 flux- and mole fraction-ratios

The vertical profiles of ER_{eco} and ER_{conc} differ temporally and spatially. Figure 4 shows the diel vertical profiles of ER^z_{eco} and ER^z_{conc} averaged over all growing seasons from 2012-2016 (between $leaf_{out}$ and $leaf_{fall\_complete}$). The mean diel ER^z_{eco} ranged from 0.985 to 1.10 mol mol^{-1} (Fig. 4a). ER^z_{eco} at the ground and bottom layers (z/ht ≤ 0.35) showed very little variability across the day reflecting the dominance of stem and soil respiration with fixed values of ER_{soil} and ER_{stem} (Fig. 4a). The upper levels of the canopy showed ER^z_{eco} between 0.99 and 1.04 mol mol^{-1} during the daylight period (6:00 to 20:00) due to the dominating fluxes of assimilation and stem respiration. The leaf dark respiration did not have a large impact on averaged daytime ER^z_{eco}. Moreover, the defined LAI and WAI distributions (Fig. 1a) were represented in the vertical profile of ER^z_{eco}, whereas the top canopy contained a larger proportion of sunlit leaves (z/ht > 0.75) than the middle part (0.35 < z/ht < 0.75). Hence, ER^z_{eco} in the top canopy was influenced more by fluxes of assimilation in daytime hours and was close to 1.00 mol mol^{-1}. Between z/ht = 0.3 and z/ht = 0.5, ER^z_{eco} was larger than 1.06 mol mol^{-1} during daytime due to higher respiratory processes than assimilation affected by low radiation and relatively high temperatures. The ER^z_{eco} during nighttime (approximately before 6:00 and after 20:00) of the upper and middle canopy was usually larger than 1.04 mol mol^{-1} due to respiratory fluxes.

The mean diel ER^z_{conc} showed relatively small variations ranging from 1.115 to 1.15 mol mol^{-1} (Fig. 4b), and thus, closely matched the prescribed atmospheric O_2:CO_2 mole fraction slope of 1.15 (Table 1). Especially during nighttime (before 6:00

https://doi.org/10.5194/bg-2023-30
Preprint. Discussion started: 2 March 2023

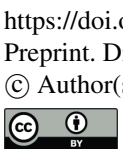

and after 20:00), ER^z_{conc} was mainly driven by the atmospheric O_2 and CO_2 background levels. However, bottom layers showed slightly lower values of ER^z_{conc}, down to 1.12 mol mol^{-1}, owing to an accumulation of CO_2 close to the soil surface produced by soil respiration and low turbulence. During daytime, the canopy air column was well mixed due to stronger turbulence. Nevertheless, ER^z_{conc} values were slightly lower in the top canopy layers towards late afternoon and sunset, caused by prevailing canopy respiration.

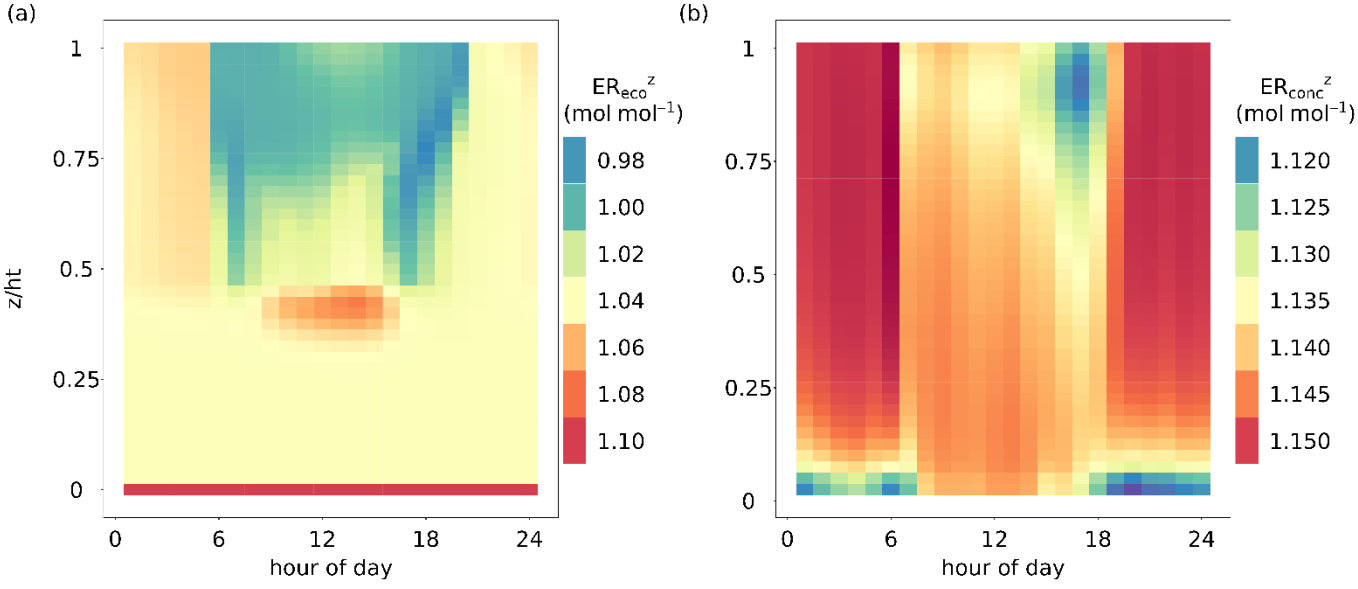

Figure 4. Comparison of the diel dynamics of the height dependent O_2:CO_2 flux- and mole fraction-ratios averaged over all growing seasons (day of year 110 to 320) from 2012 to 2016. (a) Vertical profile of the O_2:CO_2 flux-ratio inside the canopy (ER^z_{eco}, mol mol^{-1}), including the whole canopy domain and the soil component (z/ht = 0); (b) Vertical profile of the O_2:CO_2 mole fraction-ratio inside the canopy (ER^z_{conc}, mol mol^{-1}), including the whole canopy domain. The exchange ratios for specific canopy heights were derived as the slope of linear regressions fitted to O_2 and CO_2 fluxes or concentrations of multiple simulated time steps for each canopy layer.

3.4 Evaluation of the flux-gradient method to obtain O_2 fluxes

The vertical profiles of air temperature, water vapor, CO_2, and O_2 mole fractions were modeled for the entire CANVEG domain including 40 canopy layers and 80 atmosphere layers above the canopy. Figure 5 shows examples of vertical profiles for 12:00 p.m. to 13:00 p.m. (daytime) and 23:00 p.m. to 00:00 a.m. (nighttime) on 4 July 2012, an arbitrarily chosen sunny day. Generally, during daytime the vertical profiles within the canopy (Fig. 5a and 5c) were mostly induced by radiative transfer, leaf photosynthesis, transpiration and autotrophic respiration, which were influenced by the vertical LAI and WAI distributions (Fig. 1a). Furthermore, soil evaporation and respiration resulted in higher water vapor and CO_2 mole fractions close to the soil surface. For the layers above the canopy (z/ht >1), the profiles changed monotonically. Daytime O_2 and CO_2 profiles (Fig. 5c) show a mirrored shape because the O_2 and CO_2 fluxes were contributing inversely to the atmospheric mole fractions. Nighttime

https://doi.org/10.5194/bg-2023-30
Preprint. Discussion started: 2 March 2023


Biogeosciences Discussions Open Access EGU

water vapor and CO_2 profiles (Fig. 5d and 5d) show a continuous decrease with height and the O_2 profile a continuous increase, due to the dominance of soil evaporation and soil, stem and leaf respiration in the lower layers being a sink for O_2. During nighttime, air temperature (Fig. 5b) is slightly lower at the canopy top than inside the canopy due to higher energy loss by emission of longwave radiation.

Based on these modeled vertical profiles and the corresponding flux (F_{CO_2}, H or LE, respectively), O_2 fluxes were calculated with the flux-gradient method and compared to the modeled O_2 fluxes from CANVEG, both corrected for the storage term. So in the following we always describe the ecosystem fluxes (turbulent fluxes plus storage terms). Figures 5e and 5f show the difference between the various flux-gradient methods derived and modeled F_{O_2} ($diff_{F_{O_2,(c,T,v)}}$, (Eq. (7)) for the respective simulation hours, when the scalar gradients were derived from two heights (section 2.4). An F_{O_2} estimate and a $diff_{F_{O_2}}$ value were obtained for each layer. Generally, $diff_{F_{O_2}}$ derived with the flux-gradient method based on the CO_2 profile ($diff_{F_{O_2},c}$) was lower than $diff_{F_{O_2}}$ derived from the temperature and water vapor profile ($diff_{F_{O_2},T}$, $diff_{F_{O_2},v}$; Fig. 5e and 5f). For daytime conditions (Fig. 5e), the mean $diff_{F_{O_2},c}$, $diff_{F_{O_2},T}$ and $diff_{F_{O_2},v}$ above the canopy were 0.030 ± 0.09 µmol m^{-2} s^{-1}, 1.55 ± 0.54 µmol m^{-2} s^{-1} and -4.26 ± 0.63 µmol m^{-2} s^{-1}, respectively. There is little vertical variation in $diff_{F_{O_2}}$ above the canopy for nighttime (Fig. 5f). Here, the mean $diff_{F_{O_2},c}$, $diff_{F_{O_2},T}$ and $diff_{F_{O_2},v}$ were -0.53 ± 0.04, -1.98 ± 0.20 and -0.47 ± 0.24 µmol m^{-2} s^{-1}, respectively. By applying the three-heights flux-gradient method after Faassen et al. (2022), $diff_{F_{O_2}}$ for the daytime hour had a similar magnitude for $diff_{F_{O_2},c}$ with -0.13 µmol m^{-2} s^{-1} and for $diff_{F_{O_2},v}$ with -4.31 µmol m^{-2} s^{-1}, and was larger for $diff_{F_{O_2},T}$ with 4.72 µmol m^{-2} s^{-1}. The corresponding nighttime $diff_{F_{O_2},c}$, $diff_{F_{O_2},T}$ and $diff_{F_{O_2},v}$ derived from the three-heights flux-gradient method were -0.50, -2.41 and -0.66 µmol m^{-2} s^{-1}, indicating the similar $diff_{F_{O_2},c}$ and $diff_{F_{O_2},v}$, but a larger magnitude of $diff_{F_{O_2},T}$ than with two-heights flux-gradient method.

The $diff_{F_{O_2}}$ within the canopy during daytime increased and was highly variable for all three methods due to the presence of sources and sinks, and non-linearity of the gradients (Fig. 5e). $diff_{F_{O_2},c}$ and $diff_{F_{O_2},T}$ showed hyperbolic shapes with very low (< -50 µmol m^{-2} s^{-1}) and high values (> 50 µmol m^{-2} s^{-1}) where the CO_2 concentrations or the temperatures, respectively, were very close to the conditions at the top measurement height, and so the gradients were very small. The sudden jumps from large positive to large negative values were caused by the change in signs of Δc and ΔT.

To guarantee a large gradient, the height with z/ht = 2 and z/ht = 1.05 were finally used in inferring F_{O_2} from vertical CO_2, temperature and water vapor gradients. Figures 6a, 6b, and 6c show the median diel courses of $diff_{F_{O_2},c}$, $diff_{F_{O_2},T}$ and $diff_{F_{O_2},v}$ for all growing seasons from 2012-2016. Assuming that with these heights the gradients are large enough, the inferred F_{O_2} agreed well with modeled F_{O_2} for $diff_{F_{O_2},c}$ throughout the median diel course ranging from -0.45 to -0.15 µmol m^{-2} s^{-1} (Fig. 6a). The medians of $diff_{F_{O_2},T}$ and $diff_{F_{O_2},v}$ indicated that $F_{O_2,T}$ was overestimated by up to 1.59 µmol m^{-2} s^{-1} and $F_{O_2,v}$ underestimated by up to 5.43 µmol m^{-2} s^{-1} during daytime hours (Fig. 6b and 6c). The standard deviations of $diff_{F_{O_2}}$ reflected

https://doi.org/10.5194/bg-2023-30
Preprint. Discussion started: 2 March 2023


Biogeosciences Discussions Open Access EGU

the diel variation of turbulent conditions and vertical gradients, which are also dependent on the eddy diffusivity. The nighttime standard deviation of $diff_{F_{O_2},v}$ was relatively large, but smaller for $diff_{F_{O_2},T}$. The latter produced more outliers during daytime, especially during times of sunrise and sunset. The standard deviation of $diff_{F_{O_2},c}$ was relatively low and usually < 10 µmol m^{-2} s^{-1} across all times of the day except at 08:00, 12:00 and 19:00 o'clock (Fig. 6a).

The above analysis evaluates the flux-gradient method solely regarding the characteristics and dynamics of various scalar gradients. Moreover, accurate and precise measurements of the scalars are also necessary for a satisfactory performance of this method. We added a random uncertainty to our modeled O_2 mole fractions to simulate gradient measurements with the current instrument uncertainty (Δo in Eq. (6)). Figure 6d shows the distribution of the differences ($\sigma_{F_{O_2}}$) between the F_{O_2} estimates based on the flux-gradient method including a random measurement error in Δo or not. For this analysis, only hourly timesteps within all growing seasons from 2012-2016 were chosen with $\Delta o \geq 1$ ppm, when O_2 concentration increased with decreasing height above the canopy due to prevailing gross assimilation during daytime. The median of resulting $\sigma_{F_{O_2}}$ was 0.20 µmol m^{-2} s^{-1} and thus very close to zero. Here, we extracted the 10% and 90% quantile of $\sigma_{F_{O_2}}$ = -14.2 and 14.5 µmol m^{-2} s^{-1}. Thus, we used 15 µmol m^{-2} s^{-1} as the upper limit of $\sigma_{F_{O_2}}$ in the evaluation of the flux partitioning approach (section 3.5).

https://doi.org/10.5194/bg-2023-30
Preprint. Discussion started: 2 March 2023

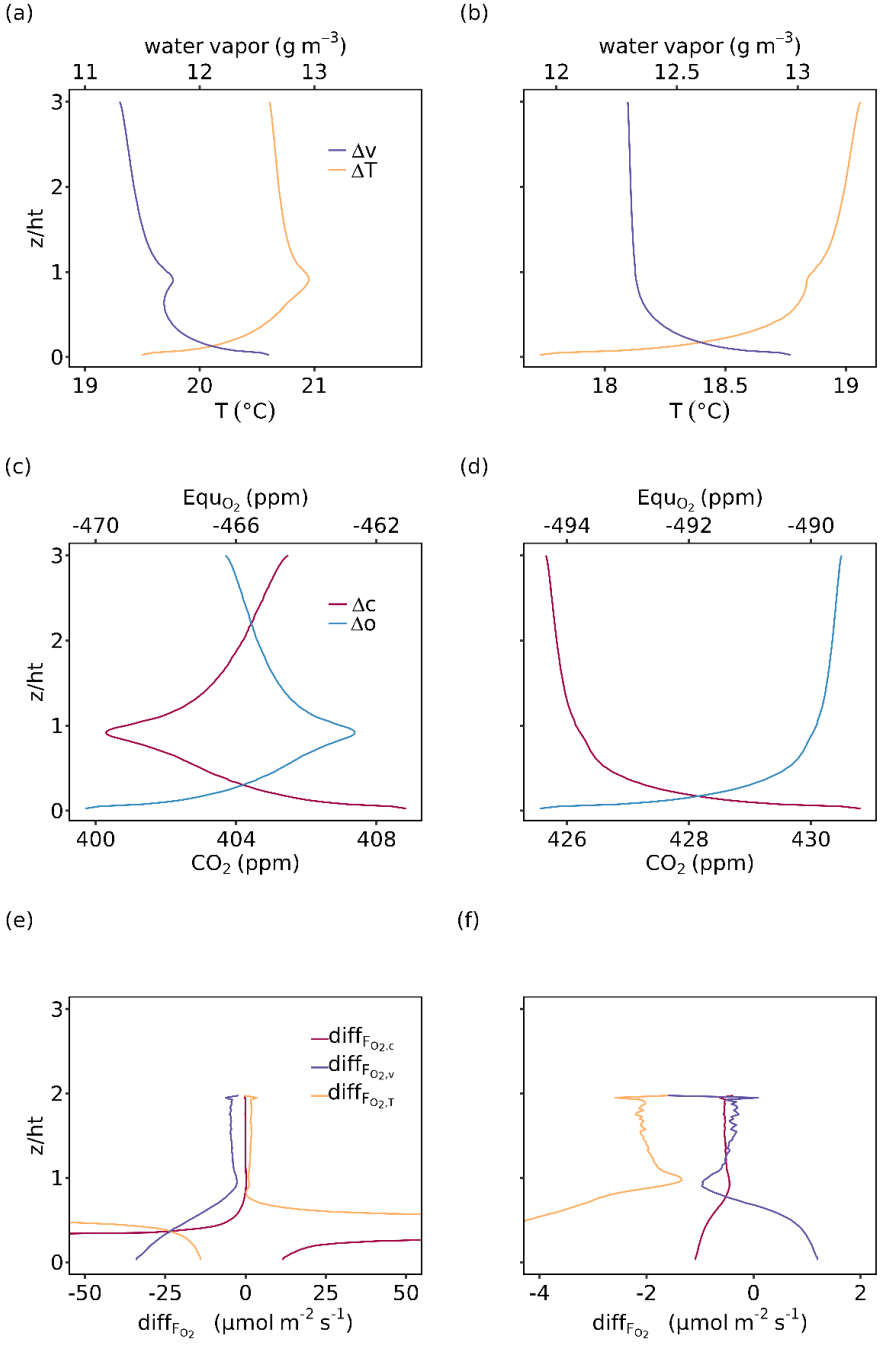

Figure 5. Vertical profiles of (a), (b) air temperature (T) and water vapor, and (c), (d) CO_2 and O_2 mole fractions of the entire model domain, where O_2 mole fractions are shown as the difference from 209750 ppm (Equ_{O_2}). (e), (f) $diff_{F_{O_2}}$ that resulted from Eq. (7) (section 2.4). The left panels (a), (c) and (e) show mean profiles for 12:00 p.m. to 13:00 p.m. (daytime) and the right panels (c), (d) and (f) for 23:00 p.m. to 00:00 a.m. (nighttime), all for 4 July 2012. The flux-gradient method was applied for the gradients between

https://doi.org/10.5194/bg-2023-30
Preprint. Discussion started: 2 March 2023

Biogeosciences Discussions Open Access EGU

a top measurement height at z/ht = 2 and each layer below, and based on profiles and fluxes of CO_2, H and LE ($diff_{F_{O_2},c}$, $diff_{F_{O_2},T}$ and $diff_{F_{O_2},v}$).

480

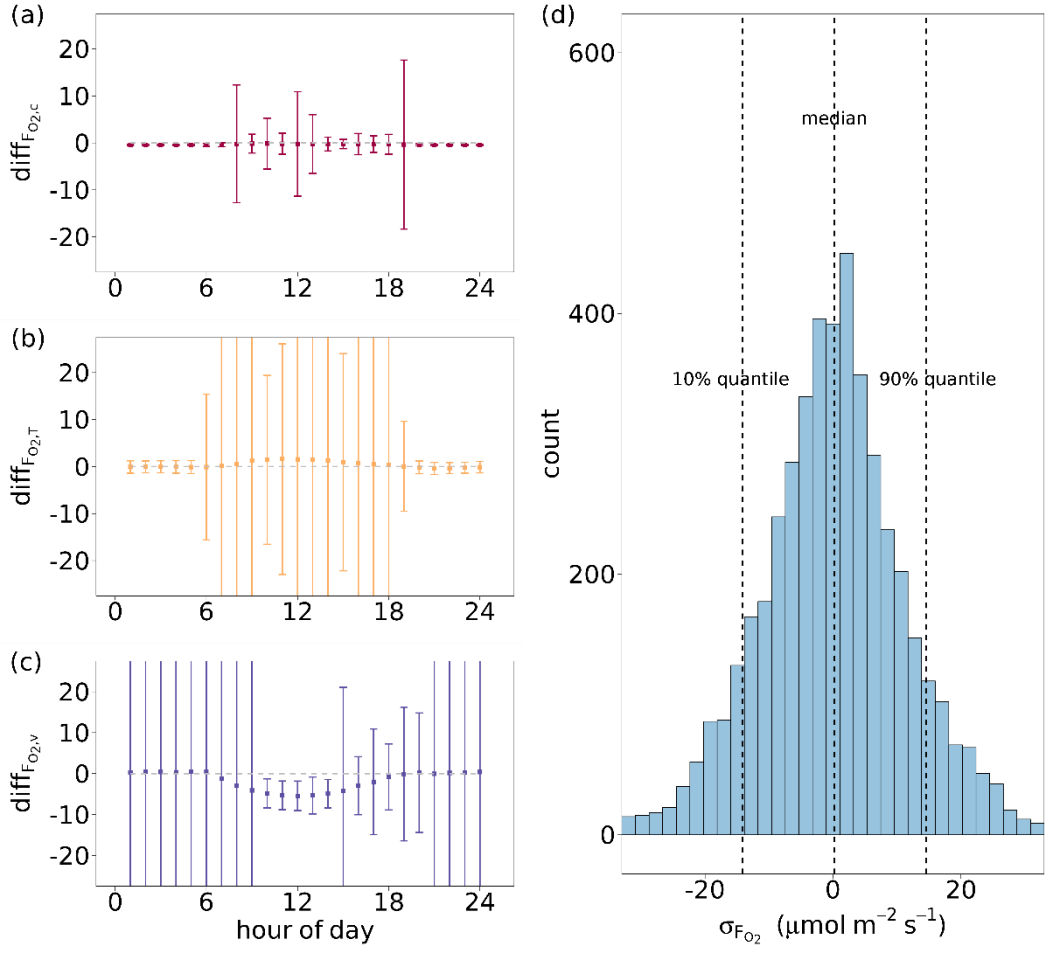

Figure 6. (a), (b), (c) Median diel cycles of the differences between O_2 fluxes derived by flux-gradient method and by CANVEG simulation ($diff_{F_{O_2}}$) for all growing seasons from 2012-2016. The flux-gradient method was applied for the gradients between z/ht = 2 and z/ht = 1.05, and based on profiles and fluxes of (a) CO_2, (b) H and (c) LE ($diff_{F_{O_2},c}$, $diff_{F_{O_2},T}$ and $diff_{F_{O_2},v}$). The error bars 485 **indicate the standard deviation of $diff_{F_{O_2}}$ by hour. (d) Histogram of uncertainties in F_{O_2} ($\sigma_{F_{O_2}}$) derived by the flux-gradient method based on CO_2 profile and fluxes, when a random uncertainty in the vertical gradient in O_2 mole fractions (Δo) was included. The uncertainty in Δo followed a normal distribution with mean = 0 and a standard deviation of 0.7 ppm (Pickers et al., 2017). In order to include daytime hours with an active canopy, $\Delta o \geq 1$ ppm was used as a filter, assuming higher oxygen concentration close to the canopy than in the top domain layers.**

490

https://doi.org/10.5194/bg-2023-30
Preprint. Discussion started: 2 March 2023

Biogeosciences Discussions

3.5 Uncertainties in partitioning net ecosystem CO_2 fluxes based on O_2 fluxes

For the test day from 07:00 to 19:00 on 4 July 2012, model output of hourly F_{O_2} was used to derive the main CO_2 flux components. The a posteriori uncertainties on the partitioned fluxes of gross assimilation (σ_{F_A}) decreased significantly with decreasing uncertainties of σ_{ER_A} and $\sigma_{F_{O_2}}$, indicating the importance of reducing errors in ER and O_2 flux measurements (Fig. 7). The a priori uncertainties had strong effects on a posteriori uncertainties, because a large $\sigma_{F_A^b}$ allowed large $|F_A - F_A^b|$ to reach a minimum J value and vice versa (Eq. (8)). Without the constraints of a priori uncertainties (Fig. 7a), σ_{F_A} reached 193 μmol m^{-2} s^{-1} at its maximum, then reduced with smaller $\sigma_{F_{O_2}}$ and σ_{ER_A} to 28 μmol m^{-2} s^{-1}, which was still larger than the a priori value (Table 2). If a priori uncertainties ($\sigma_{F_A^b}$, $\sigma_{F_R^b}$, $\sigma_{ER_A^b}$, $\sigma_{ER_R^b}$) were included (Fig. 7b and 7c), σ_{F_A} was much lower. When assuming an uncertainty for the net CO_2 fluxes ($\sigma_{F_{CO_2}}$) of 2.5 μmol m^{-2} s^{-1}, σ_{F_A} showed very little variation and ranged between 4.74 and 4.88 μmol m^{-2} s^{-1} remaining close to the minimum of the chosen a priori uncertainty in F_A and F_R (Fig. 7b). When assuming more accurate F_{CO_2} and ER_R measurements with $\sigma_{F_{CO_2}}$ = 0.5 μmol m^{-2} s^{-1} and σ_{ER_R} = 0.001 mol mol^{-1}, σ_{F_A} was reduced to a minimum of 1.43 μmol m^{-2} s^{-1} (Fig. 7c). A moderate level of a priori uncertainties in O_2 fluxes and ER_A (bold black lines in Fig. 7c) resulted in σ_{F_A} = 4.48 μmol m^{-2} s^{-1} for our test day. In this case, the partitioned F_A was 28.3 μmol m^{-2} s^{-1}, which was about 6% lower than the estimated gross assimilation obtained with the eddy covariance technique (F_A^b = 30.2 μmol m^{-2} s^{-1}).

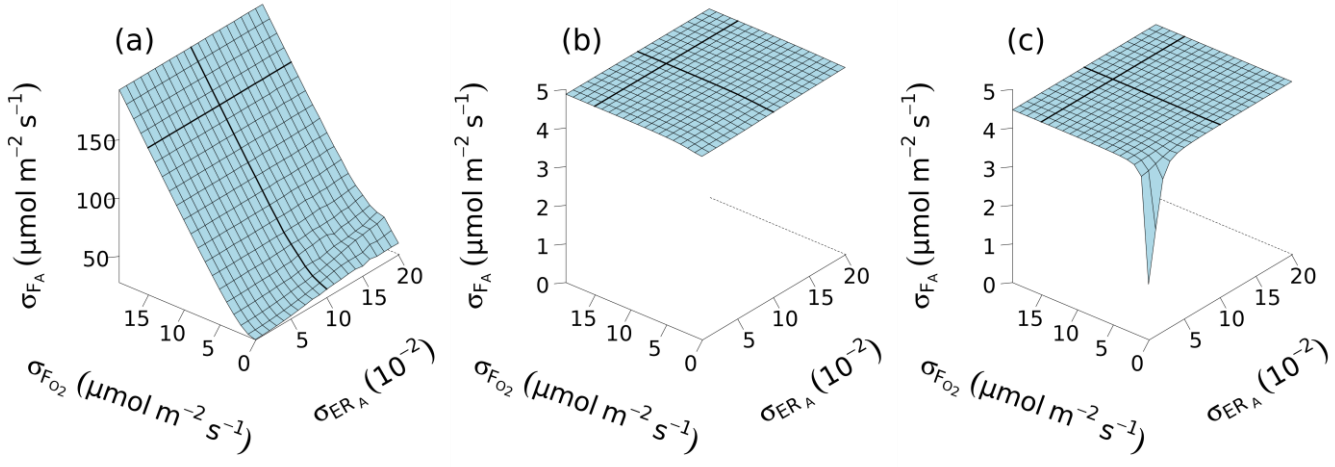

https://doi.org/10.5194/bg-2023-30
Preprint. Discussion started: 2 March 2023

Figure 7. Uncertainty in partitioned gross assimilation CO_2 flux (F_A) determined from eddy covariance net ecosystem CO_2 flux (F_{CO_2}) with net ecosystem O_2 flux (F_{O_2}), O_2:CO_2 ratio of gross assimilation (ER_A) and ecosystem respiration (ER_R) on 4 July 2012; (a) Optimized *a posteriori* uncertainty of F_A (σ_{F_A}) without *a priori* F_A values and uncertainties; (b) Optimized σ_{F_A} including all of the *a priori* terms in the J function as written in Eq. (8), with *a priori* uncertainty of F_{CO_2} ($\sigma_{F_{CO_2}}$) = 2.5 µmol m^{-2} s^{-1} and *a priori* uncertainty of ER_R ($\sigma_{ER_R^b}$) = 0.05 mol mol^{-1}; (c) Same cost function as for (b) but with $\sigma_{F_{CO_2}}$ = 0.5 µmol m^{-2} s^{-1} and $\sigma_{ER_R^b}$ = 0.001 mol mol^{-1}. The bold black lines show the practical optimization test with $\sigma_{ER_A^b}$ and $\sigma_{F_{O_2}}$ around 0.01 mol mol^{-1} and 15 µmol m^{-2} s^{-1}, respectively (cf. Figure 6d).

4 Discussions

4.1 Model set-up and model performance

We added O_2:CO_2 exchange ratios and O_2 flux processes into the one-dimensional, multi-layer atmosphere-biosphere gas exchange model, CANVEG. To represent natural atmosphere-ecosystem exchange satisfactorily, we first calibrated and validated the model based on eddy covariance CO_2 and energy flux observations from a temperate deciduous forest in Leinefelde, Germany, from 2012-2016. In a previous study, model performance was evaluated based on hourly CO_2, water vapor and energy fluxes in temperate oak forests (Baldocchi and Wilson, 2001). That evaluation, for hourly F_{CO_2}, yielded a slope = 1.09 of the regression between observations and simulation with an R^2 = 0.82, which is comparable to our results (slope = 1.02 and R^2 = 0.82, Fig. 2b). The model application in a deciduous temperate forest in central Germany (Knohl and Baldocchi, 2008) also showed a high match between hourly modeled and measured F_{CO_2} (slope = 0.997, R^2 = 0.857). In addition, Hanson et al. (2004) compared the CANVEG model with seven other stand-level models where CANVEG performed very well (slope = 0.93, R^2 = 0.82) based on simulated F_{CO_2}. In our study, the comparison between hourly LE simulation and observations obtained a regressed slope = 1.02 and R^2 = 0.77 (Fig. 2f), indicating a better model performance than for daily evapotranspiration by Hanson et al. (2004) (slope = 1.17, R^2 = 0.73). Knohl and Baldocchi (2008) found a slope = 0.926 and R^2 = 0.825 for hourly LE simulation, and a slope = 1.021 and R^2 = 0.869 for hourly H simulation, indicating an underestimation of LE and a small overestimation of H. In our study, we observed an overestimation of LE and underestimation of H. The model performance in the energy fluxes was generally lower than for CO_2 flux simulations because fitted parameters mainly affected the CO_2 fluxes and leaf assimilation (Table 1). By adjusting the assimilation rate, only transpiration was also changed, which then had an impact on LE and H. The non-unity slope of H and LE could also point to the non-closure of the energy balance in the eddy covariance observations.

Furthermore, the modeling error could be caused by the implemented soil respiration algorithm, which did not consider the influence of soil water changes. Moreover, parameters for soil respiration were only calibrated based on eddy covariance observations (F_{CO_2} and F_R) on ecosystem scale, where independent chamber measurements would be beneficial. Moreover, an error in the seasonality of carbon and energy fluxes could be introduced by the uncertainty in leaf growth phenology and annual LAI. Although we simulated fluxes from 2012 to 2016, the total leaf-full LAI and leaf growth phenology parameters (Table

https://doi.org/10.5194/bg-2023-30
Preprint. Discussion started: 2 March 2023

1) were only measured in the year 2015 and kept constant across the modeling period (Table 1). Adjusting LAI annually would only affect the timing of the fluxes, but not the overall O_2:CO_2 exchange ratio (ER) pattern.

This study used fixed ER parameter values owing to the lack of direct chamber O_2 and CO_2 flux measurements for leaf, stem and soil flux components at our study site. The O_2:CO_2 exchange ratio of gross assimilation (ER_A) was set to 1.00 mol mol^{-1} (Table 1), describing the production of carbohydrates by gross assimilation. Busch et al. (2018) described how plants use nitrogen while assimilating CO_2, resulting in carbon loss from the photorespiratory pathway in the form of glycine and serine. Since nitrogen assimilation increases O_2 emissions but has smaller effects on CO_2 uptake, incorporating nitrogen assimilation in the Farquhar et al. (1980) photosynthesis model would help to represent photosynthetic O_2 emissions more mechanistically in models. In this case, environmental conditions such as nitrogen fertilization and utilization would cause different ER_A values.

Studies obtaining exchange ratios of O_2 and CO_2 via chamber measurements at the soil- or stem-scale often state the so-called apparent respiratory quotient (ARQ), which is defined as the ratio of CO_2 efflux to O_2 uptake (Angert et al., 2012; Helm et al., 2021; Hilman and Angert, 2016; Hilman et al., 2022). Thus, ARQ could be compared to our ER_{soil} or ER_{stem} by taking the inverse of ARQ, which is the CO_2:O_2 conductance ratio, following Hilman and Angert (2016). However, ARQ is also influenced by biotic and abiotic non-respiratory processes such as dissolution and refixation of respired CO_2 in the xylem sap (Angert et al., 2012; Hilman and Angert, 2016; Hilman et al., 2022), so we expect differences between the various quantities. Furthermore, studies state the so-called oxidative ratio (OR) based on the elemental analysis of organic material. OR is based on the stoichiometry of the respiratory product or net synthesized biomass, which represents the oxidation state of respiratory substances (Hilman et al., 2022; Juergensen et al., 2021).

All ARQ values from the cited references were converted to ER_{stem} or ER_{soil} for easier comparison. The ER_{stem} parameter = 1.04 mol mol^{-1} used in this study was derived by Randerson et al. (2006) based on the OR of chemical compositions (lipid, lignin, protein, soluble phenolic etc.) assigned to woody stems. Hilman and Angert (2016) measured a mean ER_{stem} = 1.47 mol mol^{-1} (ARQ = 0.68 ± 0.04 mol mol^{-1}) with direct continuous measurements for an apple tree. In addition, ER_{stem} also showed variations between 1.22 and 1.61 mol mol^{-1} (ARQ = 0.62 to 0.82 mol mol^{-1}) during the measurement period (Hilman and Angert, 2016). The ER_{stem} varies between 1.28 and 2.56 mol mol^{-1} (ARQ = 0.39 to 0.78 mol mol^{-1}) with the mean of 1.69 mol mol^{-1} (ARQ = 0.59 mol mol^{-1}) among tropical, temperate, and Mediterranean forests (Hilman et al., 2019). Besides, dry or wet environmental conditions lead to a seasonal variation in ER_{stem} (Angert et al., 2012).

The global OR of soils is suggested to be equal 1.10 ± 0.05 (Severinghaus, 1995). According to Hockaday et al. (2015), the soil OR is 1.006 at ambient CO_2 level and increases to 1.054 with elevated CO_2 level. (Worrall et al., 2013) also derived a global soil OR = 1.04. Seibt et al. (2004) obtained an ER_{soil} = 0.94 mol mol^{-1} with field chamber measurements, while Ishidoya et al. (2013) obtained ER_{soil} = 1.11 mol mol^{-1}. ER_{soil} also showed seasonal variations from about 1.11 mol mol^{-1} (ARQ = 0.9 mol mol^{-1}) during late spring and summer to about 1.43 mol mol^{-1} (ARQ = 0.7 mol mol^{-1}) during winter in a Mediterranean mixed conifer forest (Hicks Pries et al., 2020). Depending on ecosystem type, such as alpine areas, temperate, Mediterranean or tropical forests, and on sampling strategies, such as sampling of soil air or bulk soil, obtained ER_{soil} varied between 0.88 to 4.35 mol mol^{-1} (ARQ = 0.23 to 1.14 mol mol^{-1}) (Angert et al., 2015; Angert et al., 2012; Hilman et al., 2022). These variabilities

https://doi.org/10.5194/bg-2023-30
Preprint. Discussion started: 2 March 2023

related to seasons, forest types and ecosystem processes highly indicate that site specific ER_{stem} and ER_{soil} should be used in O_2 flux simulations. A logarithmic relationship between soil ARQ and soil temperature, as found by Hilman et al. (2022), could also be introduced to future soil O_2 flux models.

Due to this high variance between derived ER of these different studies, we conducted a sensitivity analysis by changing ER_A, ER_{stem} or ER_{soil} by ± 10% to show how these parameters affected the modeled F_{O_2}. If ER_A was increased or decreased by 10%, the modeled F_{O_2} sum of the entire study period increased or decreased on average by 18.6% correspondingly. Similarly, a change by a 10% increment on ER_{soil} and ER_{stem} caused the F_{O_2} sum to increase or decrease by 6.9% and 1.7%, respectively. These results directly followed Eq. (1) where the derivative with respect to a specific ER gives the corresponding flux in percent. Oxygen fluxes are hence most sensitive to the ER of the largest carbon fluxes.

4.2 Temporal and vertical dynamics of O_2:CO_2 exchange ratios

The O_2:CO_2 flux exchange ratio (ER_{eco}) quantifies the simultaneous canopy-atmosphere gas exchange of the whole ecosystem. We obtained ER_{eco} by aggregating simulated O_2 and CO_2 fluxes of all canopy layers and taking the ratio or by deriving the slopes of linear regressions fitted to O_2 and CO_2 fluxes of multiple simulated time steps for each canopy layer (ER^z_{eco}). The variations in ER_{eco} were evoked by diel and seasonal variations in the flux contributions of gross assimilation and respiration to net ecosystem O_2 and CO_2 exchange. Since assimilation and respiration are two individual processes but they have - corresponding to their respective main drivers, photosynthetic photon flux density and temperature - shifted diel cycles. Furthermore, fluxes of respiration consist of various components originating from various sources (e.g., respiration by heterotrophs, leaves or roots), which can also differ in their diel cycles, in their ER and in their proportions of total O_2 and CO_2 ecosystem fluxes. Further studies should obtain ER independently with respective chamber measurements in order to separate environmental effects (e.g., radiation, temperature, humidity) on each componential O_2 and CO_2 fluxes.

The ER_{eco} contains information of the turbulent flux exchange and of the O_2 and CO_2 storage terms between soil surface and measurement height. Our study focused on the whole ecosystem O_2 and CO_2 exchange ratio including storage terms. Annual mean ER_{eco} ranged from 1.06 to 1.12 mol mol^{-1} within the five years and estimates of ER^z_{eco} varied between 0.99 and 1.10 mol mol^{-1} with height in the canopy (Fig. 4a). Seibt et al. (2004) reported daytime net turbulent ER (considering turbulent fluxes and not including storage terms) between 1.26 and 1.38 mol mol^{-1}, which they derived with a one-box model. Next to the in- or exclusion of storage terms and the usage of different models, differences between our studies could also be caused by the difference in considered time periods: our simulations covered five years' growing seasons of O_2 and CO_2 fluxes between the canopy and the atmosphere, and Seibt et al. (2004) focused on July and August between 1999 and 2001. Moreover, we used different componential ER parameters (Table 1) in our simulations.

Diel ER_{An} variations reflected separate responses of gross assimilation and leaf dark respiration to temperature. The median and mean of hourly ER_{An} were 0.99 and 0.96 mol mol^{-1}, respectively, for all growing seasons during the study period. However, ER_{An} showed extreme values during transition hours with low flux magnitudes (Fig. 3b). Ishidoya et al. (2013) found ER_{An}

https://doi.org/10.5194/bg-2023-30
Preprint. Discussion started: 2 March 2023

values close to 1.02 mol mol^{-1} via leaf chamber measurements. According to Seibt et al. (2004), ER_{An} ranged between 1.04 and 1.20 mol mol^{-1} observed also via chamber measurements when flux rates are between 2 and 5 µmol m^{-2} s^{-1}. A lower flux rate (1.7 µmol m^{-2} s^{-1}) leads to a higher variability in ER_{An} (Seibt et al., 2004). The divergence between our ER_{An} estimates (which were close to 1.00 mol mol^{-1}) and to the chamber measurements could be caused by the synthesis of varying nitrogen sources that would increase ER_{An} (Seibt et al., 2004).

The mole-based O_2:CO_2 exchange ratio (ER_{conc}) is determined by the atmospheric background concentrations of O_2 and CO_2, by the distributions and dynamics of sources and sinks and the turbulence inside the canopy. ER_{conc} is usually derived based on the slopes of Deming regressions of observed O_2 and CO_2 mole fractions accounting for uncertainty in both variables (Battle et al., 2019; Ishidoya et al., 2020). Our results of ER_{conc} and ER_{eco} confirmed that ER_{conc} cannot represent simultaneous O_2 and CO_2 exchange as ER_{eco}, which was also recently found (Faassen et al., 2022). We also estimated ER^z_{conc} for each canopy layer representing O_2 and CO_2 mole fractions of air on certain canopy heights. The mean diel ER^z_{conc} showed only very small variations ranging from 1.12 to 1.15 mol mol^{-1} within the diel course. Battle et al. (2019) observed an average ER_{conc} = 1.081 ± 0.007 mol mol^{-1} in a mixed deciduous forest over a six years' period and ER_{conc} = 1.03 ± 0.01 mol mol^{-1} on two summer days in July 2007. Their ER_{conc} measurements also showed temporal variations on a 6-hour basis between 0.85 and 1.15 mol mol^{-1}. Seibt et al. (2004) measured and modelled ER_{conc} during day- and nighttime at several sites and obtained values varying between 1.04 and 1.19 mol mol^{-1}. Ishidoya et al. (2013) observed daily average ER_{conc} = 0.94 ± 0.01 mol mol^{-1}, with daytime ER_{conc} = 0.87 ± 0.02 mol mol^{-1} and nighttime ER_{conc} = 1.03 ± 0.02 mol mol^{-1}. Ishidoya et al. (2013) also built a one-box canopy O_2/CO_2 budget model applying the same parameter values ER_A = 1.00 mol mol^{-1} and ER_R = 1.10 mol mol^{-1} as our study. Their observed daytime ER_{conc} = 0.87 mol mol^{-1} agrees with their modeled net turbulent ER = 0.89 mol mol^{-1}. Our modeled ER^z_{conc} estimates showed a lower temporal variability within the mean diel course than in the cited studies. This is to a large part due to background O_2 that was fixed to 1.15 of atmospheric CO_2 concentrations (Table 2). One would expect, though, that this ratio might be lower during summer and most probably has also a diel cycle. Future work could include continuous measurements at the site resulting in a varying background value and potentially larger diel and seasonal variability. It is also possible that mixing in CANVEG was too strong so that modeled ER^z_{conc} was too influenced by the background value. This could be improved in future by comparing modelled temperature, H_2O and CO_2 concentrations with measured concentrations in different canopy heights, which become standard measurements at eddy covariance sites on forests now.

4.3 Estimation of ecosystem O_2 fluxes and applications

Eddy covariance measurements, as typically conducted for CO_2 fluxes, are currently not possible for O_2 fluxes, because no sufficiently fast and precise O_2 analyzer is commercially available, yet (except for a self-made, non-commercial vacuum ultraviolet (VUV) absorption analyzer developed by Stephens et al. (2003)). Requirements would be a precision of below 1 ppm against a background concentration of 210 000 ppm on a high, turbulence resolving measurement frequency (Keeling and Manning, 2014). However, vertical profiles of air temperature, water vapor, CO_2 and O_2 mole fractions can already be obtained with high precision. With our modeled vertical profiles, we determined O_2 fluxes based on the flux-gradient approach, testing

https://doi.org/10.5194/bg-2023-30
Preprint. Discussion started: 2 March 2023

various profile set-ups and the necessary instrument precision for O_2 concentration measurements (Fig. 5 and 6). By choosing various heights to derive the mole fraction gradients, we could confirm that the selected heights should be both above the canopy. This guarantees that the profiles are differentiable as there are no sources or sinks between sampling heights, and that the eddy diffusivity of O_2 is the same as of the other corresponding scalars (Baldocchi et al., 1988). In addition, the mole fraction difference between the two heights should be as large as possible to decrease the uncertainty in O_2 flux estimates. Here, we selected amongst others heights at z/ht = 1.05 and = 2 to obtain large gradients. Faassen et al. (2022) applied the flux-gradient method to estimate O_2 fluxes in a boreal forest with a canopy height = 18 m. Their measurements were conducted between 23 m and 125 m for the vertical scalar gradient, reaching about seven times the canopy height. Such a large distance between measurement heights in a profile system is usually only feasible for cropland, grassland or peatland study sites with low vegetation. For high vegetation, such as forest sites, a tall tower is needed (as in Faassen et al., 2022). However, by choosing two measurement heights with a large distance (e.g., multiple tens of meters), the difference between the footprint extensions of each height becomes also large, potentially resulting in erroneous flux estimates. If, for instance, the vertical CO_2 gradient could be doubled, the error in F_{O_2} fluxes caused by the measurement error of O_2 gradients would be reduced by 50% according to Eq. (6).

The median differences between F_{O_2} derived with the flux-gradient method and modeled F_{O_2} ($diff_{F_{O_2}}$) were generally < 5.5 µmol m^{-2} s^{-1}, independent of which scalar concentrations and fluxes were used for the latter. However, $diff_{F_{O_2},v}$ and $diff_{F_{O_2},T}$ deviated more from zero during daytime, indicating that F_{O_2} estimates based on LE and water vapor profile and H and temperature profile would lead to underestimation or overestimation, respectively, during daytime by the flux-gradient method (Fig. 6). The F_{O_2} estimates during nighttime were more uncertain based on temperature and water vapor, as indicated by large standard deviations. These "outliers" occurred due to too small vertical gradients, caused by a small activity of sources and sinks and/or of insufficient turbulence. The flux-gradient method based on CO_2 concentrations and fluxes yielded F_{O_2} estimates in better agreement with modeled F_{O_2}. But this was probably because the O_2 sources and sinks were highly correlated to CO_2 processes due to the O_2 modeling set-up and constant ER (Eq. (1)). Consequently, it is still recommended to use all the available gas or energy gradients to derive O_2 fluxes with the flux-gradient methods, and then choose the most appropriate method (if this is possible) for various times during the day or year depending on the magnitude of the gradients, the quality of flux measurements and the turbulence. The magnitude of the gradients could additionally be increased for each scalar by choosing scalar-specific measurement heights.

The flux-gradient method has already been used for O_2 flux estimation above a cool temperate forest (Ishidoya et al., 2015), an urban canopy (Ishidoya et al., 2020) and a boreal forest (Faassen et al., 2022). The latter study applied a three-heights flux gradient approach, where they estimated the eddy diffusivity K based on CO_2 and temperature measurements at three heights and applied a vertical O_2 gradient between two heights. We also tested here this three-heights flux gradient approach based on our model simulations, but we assumed that all scalars including O_2 were measured at three heights. Based on our simulations,

https://doi.org/10.5194/bg-2023-30
Preprint. Discussion started: 2 March 2023

we could not observe an improvement of the flux estimation due to the inclusion of three measurement heights in the flux-gradient method instead of two heights.

Uncertainty on O_2 mole fraction estimates resulted in a median close to zero for the uncertainty $\sigma_{F_{O_2}}$. The uncertainty in O_2 concentration estimates were selected randomly following a normal distribution in the model simulations. Our analysis showed that the flux-gradient method has the potential for F_{O_2} estimation, but we also found that estimated F_{O_2} could be over- or underestimated by up to ±5.5 µmol m^{-2} s^{-1}. To make the flux-gradient method more precise, the vertical scalar gradient should be as large as possible and flux and profile measurements as precise as possible. To achieve this, on the one hand, a larger distance between measurement heights is needed (not possible over large forest stands, but applicable for crop-, grass-, and peatland), and on the other hand, a higher measurement precision is necessary to reduce the uncertainty in scalar gradient measurements.

F_{CO_2} obtained with the eddy covariance technique was source partitioned based on simulated F_{O_2} and the uncertainty in gross assimilation (σ_{F_A}) was evaluated. By estimating CO_2 flux components following the same approach based on stable isotopes in CO_2, Knohl and Buchmann (2005) derived a σ_{F_A} for instantaneous half-hourly data of 6 µmol m^{-2} s^{-1} assuming CO_2 and $^{13}CO_2$ flux uncertainties of 0.5 µmol m^{-2} s^{-1} and 25‰ µmol m^{-2} s^{-1}, respectively. A σ_{F_A} of around 4 µmol m^{-2} s^{-1} was found with a higher uncertainty in CO_2 fluxes ($\sigma_{F_{CO_2}}$) = 2 µmol m^{-2} s^{-1} by Ogee et al. (2004). Our study obtained comparable results under similar $\sigma_{F_{CO_2}}$ = 2.5 µmol m^{-2} s^{-1} (Fig. 7b). However, Ogee et al. (2004) found that σ_{F_A} can be reduced to 2 µmol m^{-2} s^{-1} when an isotopic disequilibrium is larger than 0.004 (Fig. 6 in Ogee et al. (2004), page 11). We obtained ER_A and ER_R disequilibrium ($|ER_A - ER_R|$) of around 0.086 mol mol^{-1}, but still could not improve our σ_{F_A} under normal $\sigma_{F_{CO_2}}$ level (Fig. 7b). This was probably because our uncertainty in O_2 fluxes ($\sigma_{F_{O_2}}$) was much larger (up to 15 µmol m^{-2} s^{-1}) relative to the ER_A and ER_R disequilibrium (0.086 mol mol^{-1}) (Ogee et al., 2004). Here, we derived $\sigma_{F_{O_2}}$ based on the analysis of the flux-gradient application (Fig. 6d). Thus, a higher precision in F_{O_2} estimates and/or a larger ER_A and ER_R disequilibrium ≥ 0.086 mol mol^{-1} is needed. In our simulations, the disequilibrium had low variation due to the fixed ER parameters. A small variation was only introduced by the variable ER_{rd} due to leaf temperature. By implementing variable ER parameters (depending on environmental conditions etc.) in the model or obtaining real ER values by measurements could be beneficial. Figure 7c showed that by improving the precision in F_{CO_2} and ER_R estimates and not so much in F_{O_2} also yields a lower uncertainty in estimates of gross assimilation. Faassen et al. (2022) changed ER_{eco} by ±0.20 mol mol^{-1}, which resulted in a change in partitioned F_A of 6.7%. However, they compared their partitioned flux components with F_A and F_R derived by the eddy covariance method, by assuming that the latter describes the "true" values. They emphasize the importance of a correct estimate for ER_{eco}. Our evaluation of σ_{F_A} was based on assigned a priori uncertainties to all elements which were independent of the flux values (Ogee et al., 2004). Compared with eddy covariance data, our partitioned F_A also differed by about 6% which is comparable to flux partitioning results by Faassen et al. (2022).

https://doi.org/10.5194/bg-2023-30
Preprint. Discussion started: 2 March 2023

5 Conclusions

We implemented O_2:CO_2 exchange ratios in the CANVEG multi-layer ecosystem-atmosphere gas exchange model to enable hourly ecosystem O_2 flux simulations. The simulated ecosystem O_2:CO_2 exchange ratio (ER_{eco}) showed strong diel and seasonal variations. The annual mean ER_{eco} ranged from 1.06 to 1.12 mol mol^{-1} during the five years' study period and depended significantly on our assumptions about the fixed model parameters describing the exchange ratios of the ecosystem components: leaves, stem and soil (ER_A, ER_{stem}, ER_{soil}). We also found that hourly ER_{eco} and exchange ratios of net assimilation (ER_{An}) exhibited high variability during transition periods (e.g., during sunrise and sunset) with low flux magnitudes. According to our simulations, it is feasible to derive ecosystem O_2 fluxes with the flux-gradient approach based on sensible heat, latent heat and CO_2 turbulent flux measurements under field conditions, when the vertical gradients are measured between 1.05 to 2 times of the canopy height. Specially, the vertical O_2 gradient should be larger than 1 ppm. However, including uncertainty in O_2 mole fraction measurements by 0.7 ppm would increase the uncertainty in O_2 flux estimates up to 15 µmol m^{-2} s^{-1}. The precision of the source partitioning application was driven by a priori uncertainties of O_2 and CO_2 flux, ER_A and ER_R measurements. With an ER_A and ER_R disequilibrium ($|ER_A - ER_R|$) of about 0.086 mol mol^{-1}, the uncertainty of partitioned gross assimilation can be constrained to < 5 µmol m^{-2} s^{-1} by narrowing the uncertainty of CO_2 measurements and ER_R estimates to 2.5 µmol m^{-2} s^{-1} and 0.05 mol mol^{-1}. O_2 fluxes measurements and additional information on the exchange ratios of gross assimilation and ecosystem respiration (ER_A, ER_R), for example obtained by chamber measurements, can thus be used as a source partitioning approach for net CO_2 fluxes. Our model study highlights the potential temporal and spatially variability of O_2:CO_2 exchange ratios of various ecosystem components and the drivers of O_2 fluxes at a forest study site. Furthermore, we provided guidance to micrometeorological approaches, such as the flux-gradient method, to obtain sufficient O_2 flux estimates depending on measurement set-up and on current instrument precision. We further tested the usage of O_2 flux estimates to source partition net CO_2 fluxes. Further understanding of the relationship between environmental drivers and O_2 fluxes and O_2:CO_2 exchange ratios, and continuous and long-term observations based on for instance chamber measurements, will greatly help to improve our ecosystem model and our understanding of the carbon cycle in terrestrial ecosystems.

Acknowledgements

This research was funded by the European Research Council under the European Union's Horizon 2020 research and innovation program (grant agreement no. 682512–OXYFLUX). We acknowledge support by the Open Access Publication Funds of the Göttingen University. We thank the staff from the Bioclimatology Group of the University of Göttingen, especially Dietmar Fellert, Frank Tiedemann, Edgar Tunsch and Marek Peksa, for their continuous support in data acquisition and instrument maintenance. We thank Penelope A. Pickers, Emmanuel Blei, Julian Deventer and Mattia Bonazza for building O_2 flux instruments and providing atmospheric O_2 and CO_2 background data. We also thank Jelka Braden-Behrens for obtaining leaf area measurements, Ashehad Ali for suggestions on model parameter calibrations, Jan Muhr for interpretations

https://doi.org/10.5194/bg-2023-30
Preprint. Discussion started: 2 March 2023

735 of ER results, and Rijan Tamrakar and Christian Markwitz for preparing the meteorological and eddy covariance data. Lastly, we also thank the forest manager Ulrich Breitenstein for allowing the experimental setup at the Leinefelde site.

Appendix A

Table A1. Nomenclature and abbreviations. ** Units with m^{-2} indicate "per leaf area" (otherwise always "per ground area").

Abbreviation	Unit	Full name
ARQ	mol mol^{-1}	apparent respiratory quotient
b	µmol m^{-2} s^{-1} **	intercept of Ball-Berry model after Collatz et al. (1991)
$CO_{2\ atm}$	ppm	atmospheric CO_2 mole fraction
c_p	J kg^{-1} K^{-1}	specific heat capacity of air
$diff_{F_{O_2},x}$	µmol m^{-2} s^{-1}	difference between O_2 fluxes derived by the flux-gradient method and by model simulations. The subscript "*x*" represents the considered scalar profile (T: temperature, v: water vapor, c: CO_2 mole fraction).
DOY		day of year
Equ_{O_2}	ppm	difference of O_2 mole fraction from 209750 ppm
ER	mol mol^{-1}	O_2:CO_2 exchange ratio
ER_A	mol mol^{-1}	O_2:CO_2 exchange ratio of gross assimilation
ER_A^b	mol mol^{-1}	*a priori* mean of ER_A
ER_{An}	mol mol^{-1}	O_2:CO_2 exchange ratio of net assimilation
ER_{conc}	mol mol^{-1}	atmospheric O_2:CO_2 mole fraction ratio
ER^z_{conc}	mol mol^{-1}	height dependent atmospheric O_2:CO_2 mole fraction ratio
ER_{eco}	mol mol^{-1}	ecosystem O_2:CO_2 exchange ratio
ER^z_{eco}	mol mol^{-1}	height dependent ecosystem O_2:CO_2 exchange ratio
ER_R	mol mol^{-1}	O_2:CO_2 exchange ratio of ecosystem respiration
ER_R^b	mol mol^{-1}	*a priori* mean of ER_R
ER_{rd}	mol mol^{-1}	O_2:CO_2 exchange ratio of leaf dark respiration
ER_{soil}	mol mol^{-1}	O_2:CO_2 exchange ratio of soil respiration
ER_{stem}	mol mol^{-1}	O_2:CO_2 exchange ratio of stem respiration
F_A	µmol m^{-2} s^{-1}	gross assimilation CO_2 flux (gross carboxylation minus photorespiration)
F_A^b	µmol m^{-2} s^{-1}	*a priori* mean of F_A

https://doi.org/10.5194/bg-2023-30
Preprint. Discussion started: 2 March 2023

F_{CO_2}	µmol m^{-2} s^{-1}	net ecosystem CO_2 flux
$F_{CO_2}^z$	µmol m^{-2} s^{-1}	height dependent net ecosystem CO_2 flux
$F_{CO_2}^{\sim}$	µmol m^{-2} s^{-1}	net turbulent CO_2 flux
f_{DBH}		fraction of stem diameter to the diameter at breast height
f_{LAI}		fraction of LAI per layer
F_{O_2}	µmol m^{-2} s^{-1}	net ecosystem O_2 flux
$F_{O_2}^z$	µmol m^{-2} s^{-1}	height dependent net ecosystem O_2 flux
$F_{O_2}^{\sim}$	µmol m^{-2} s^{-1}	net turbulent O_2 flux
F_R	µmol m^{-2} s^{-1}	gross ecosystem respiration CO_2 flux
F_R^b	µmol m^{-2} s^{-1}	*a priori* mean of F_R
F_{rd}	µmol m^{-2} s^{-1}	leaf dark respiration CO_2 flux
F_{soil}	µmol m^{-2} s^{-1}	soil respiration CO_2 flux
F_{stem}	µmol m^{-2} s^{-1}	stem respiration CO_2 flux
H	W m^{-2}	net ecosystem sensible heat flux
$H^{\sim}$	W m^{-2}	net turbulent sensible heat flux
ht	m	canopy height
J		cost function
J_{max25}	µmol m^{-2} s^{-1}	maximum electron transport rate at 25 °C
k_{ball}		slope of Ball-Berry model after Collatz et al. (1991)
K_c, K_o, K_T, K_v	m^2 s^{-1}	eddy diffusivity of CO_2, O_2, heat and water vapor
LAI	m^2 m^{-2}	leaf area index
LE	W m^{-2}	net ecosystem latent heat flux
$LE^{\sim}$	W m^{-2}	net turbulent latent heat flux
$leaf_{out}$		DOY for the start of leaf growth
$leaf_{full}$		DOY for the end of leaf growth
$leaf_{fall}$		DOY for the start of leaf fall
$leaf_{fall\_complete}$		DOY for the end of leaf fall
MCMC		Markov-Chain Monte Carlo methods
$O_{2\ atm}$	ppm	atmospheric O_2 mole fraction

https://doi.org/10.5194/bg-2023-30
Preprint. Discussion started: 2 March 2023

OR		oxidative ratio
r_1, r_2		coefficients for exponential relationship between soil temperature and soil respiration
R_{d25}	μmol m^{-2} s^{-1}	leaf dark respiration at 25 °C
RMSE		root mean squared error
T	°C	air temperature
T_{leaf}	°C	leaf temperature
T_{optjm}	°C	optimum temperature for electron transport
T_{optvc}	°C	optimum temperature for maximum carboxylation
V_{cmax25}	μmol m^{-2} s^{-1} **	maximum carboxylation at 25 °C
WAI	m^2 m^{-2}	wood area index
z	m	height above the surface
α		fraction of the photosystem II activity
Δc	ppm	vertical CO_2 mole fraction gradient
Δo	ppm	vertical O_2 mole fraction gradient
ΔT	°C	vertical air temperature gradient
Δv	kg m^{-3}	vertical water vapor density gradient
Δz	m	vertical height gradient
θ_J		curvature parameter of light response curve
λ	J kg^{-1}	latent heat of vaporization
ρ_m	kg m^{-3}	air mass density
ρ_n	mol m^{-3}	air molar density
σ_{ER_A}	mol mol^{-1}	*a posteriori* uncertainty of ER_A
$\sigma_{ER_A^b}$	mol mol^{-1}	*a priori* uncertainty of ER_A
σ_{ER_R}	mol mol^{-1}	*a posteriori* uncertainty of ER_R
$\sigma_{ER_R^b}$	mol mol^{-1}	*a priori* uncertainty of ER_R
σ_{F_A}	μmol m^{-2} s^{-1}	*a posteriori* uncertainty of F_A
$\sigma_{F_A^b}$	μmol m^{-2} s^{-1}	*a priori* uncertainty of F_A
$\sigma_{F_{CO_2}}$	μmol m^{-2} s^{-1}	uncertainty of CO_2 flux estimates
$\sigma_{F_{O_2}}$	μmol m^{-2} s^{-1}	uncertainty of O_2 flux estimates

https://doi.org/10.5194/bg-2023-30
Preprint. Discussion started: 2 March 2023

σ_{F_R}	μmol m^{-2} s^{-1}	*a posteriori* uncertainty of F_R
$\sigma_{F_R^b}$	μmol m^{-2} s^{-1}	*a priori* uncertainty of F_R

References

Angert, A., Yakir, D., Rodeghiero, M., Preisler, Y., Davidson, E., and Weiner, T.: Using O_2 to study the relationships between soil CO_2 efflux and soil respiration, Biogeosciences, 12, 2089-2099, doi:10.5194/bg-12-2089-2015, 2015.

Angert, A., Muhr, J., Negron Juarez, R., Alegria Muñoz, W., Kraemer, G., Ramirez Santillan, J., Barkan, E., Mazeh, S., Chambers, J. Q., and Trumbore, S. E.: Internal respiration of Amazon tree stems greatly exceeds external CO_2 efflux, Biogeosciences, 9, 4979-4991, doi:10.5194/bg-9-4979-2012, 2012.

Anthoni, P. M., Knohl, A., Rebmann, C., Freibauer, A., Mund, M., Ziegler, W., Kolle, O., and Schulze, E. D.: Forest and agricultural land-use-dependent CO_2 exchange in Thuringia, Germany, Global Change Biol, 10, 2005-2019, doi:10.1111/j.1365-2486.2004.00863.x, 2004.

Baldocchi, D.: A Lagrangian random-walk model for simulating water vapor, CO2 and sensible heat flux densities and scalar profiles over and within a soybean canopy, Bound-Lay Meteorol, 61, 113-144, doi:10.1007/BF02033998, 1992.

Baldocchi, D.: Measuring and modelling carbon dioxide and water vapour exchange over a temperate broad-leaved forest during the 1995 summer drought, Plant Cell Environ, 20, 1108-1122, doi:10.1046/j.1365-3040.1997.d01-147.x, 1997.

Baldocchi, D., Falge, E., Gu, L. H., Olson, R., Hollinger, D., Running, S., Anthoni, P., Bernhofer, C., Davis, K., Evans, R., Fuentes, J., Goldstein, A., Katul, G., Law, B., Lee, X. H., Malhi, Y., Meyers, T., Munger, W., Oechel, W., U, K. T. P., Pilegaard, K., Schmid, H. P., Valentini, R., Verma, S., Vesala, T., Wilson, K., and Wofsy, S.: FLUXNET: A new tool to study the temporal and spatial variability of ecosystem-scale carbon dioxide, water vapor, and energy flux densities, B Am Meteorol Soc, 82, 2415-2434, doi:10.1175/1520-0477(2001)082<2415:FANTTS>2.3.CO;2, 2001.

Baldocchi, D. D. and Wilson, K. B.: Modeling CO_2 and water vapor exchange of a temperate broadleaved forest across hourly to decadal time scales, Ecol Model, 142, 155-184, doi:10.1016/S0304-3800(01)00287-3, 2001.

Baldocchi, D. D., Hincks, B. B., and Meyers, T. P.: Measuring Biosphere-Atmosphere Exchanges of Biologically Related Gases with Micrometeorological Methods, Ecology, 69, 1331-1340, doi:10.2307/1941631, 1988.

Baldocchi, D. D., Wilson, K. B., and Gu, L. H.: How the environment, canopy structure and canopy physiological functioning influence carbon, water and energy fluxes of a temperate broad-leaved deciduous forest-an assessment with the biophysical model CANOAK, Tree Physiology, 22, 1065-1077, doi:10.1093/treephys/22.15-16.1065, 2002.

Baldocchi, D. D., Fuentes, J. D., Bowling, D. R., Turnipseed, A. A., and Monson, R. K.: Scaling isoprene fluxes from leaves to canopies: Test cases over a boreal aspen and a mixed species temperate forest, J Appl Meteorol, 38, 885-898, doi:10.1175/1520-0450(1999)038<0885:SIFFLT>2.0.CO;2, 1999.

Battle, M., Bender, M. L., Tans, P. P., White, J. W. C., Ellis, J. T., Conway, T., and Francey, R. J.: Global carbon sinks and their variability inferred from atmospheric O-2 and delta C-13, Science, 287, 2467-2470, 2000.

Battle, M. O., Munger, J. W., Conley, M., Sofen, E., Perry, R., Hart, R., Davis, Z., Scheckman, J., Woogerd, J., Graeter, K., Seekins, S., David, S., and Carpenter, J.: Atmospheric measurements of the terrestrial O_2 : CO_2 exchange ratio of a midlatitude forest, Atmos Chem Phys, 19, 8687-8701, doi:10.5194/egusphere-egu22-4213, 2019.

Bowling, D. R., Tans, P. P., and Monson, R. K.: Partitioning net ecosystem carbon exchange with isotopic fluxes of CO_2, Global Change Biol, 7, 127-145, doi:10.1046/j.1365-2486.2001.00400.x, 2001.

Braden-Behrens, J., Markwitz, C., and Knohl, A.: Eddy covariance measurements of the dual-isotope composition of evapotranspiration, Agricultural and Forest Meteorology, 269, 203-219, doi:10.1016/j.agrformet.2019.01.035, 2019.

Braden-Behrens, J., Yan, Y., and Knohl, A.: A new instrument for stable isotope measurements of ^{13}C and ^{18}O in CO_2 – instrument performance and ecological application of the Delta Ray IRIS analyzer, Atmos. Meas. Tech., 10, 4537-4560, 10.5194/amt-10-4537-2017, 2017.

Busch, F. A., Sage, R. F., and Farquhar, G. D.: Plants increase CO_2 uptake by assimilating nitrogen via the photorespiratory pathway, Nature Plants, 4, 46-54, doi:10.1038/s41477-017-0065-x, 2018.

Collatz, G. J., Ball, J. T., Grivet, C., and Berry, J. A.: Physiological and environmental-regulation of stomatal conductance, photosynthesis and transpiration - a model that includes a laminar boundary-layer, Agricultural and Forest Meteorology, 54, 107-136, doi:10.1016/0168-1923(91)90002-8, 1991.

Faassen, K. A. P., Nguyen, L. N. T., Broekema, E. R., Kers, B. A. M., Mammarella, I., Vesala, T., Pickers, P. A., Manning, A. C., Vilà-Guerau de Arellano, J., Meijer, H. A. J., Peters, W., and Luijkx, I. T.: Diurnal variability of atmospheric O_2, CO_2 and their exchange ratio above a boreal forest in southern Finland, Atmos. Chem. Phys. Discuss., 2022, 1-33, 10.5194/acp-2022-504, 2022.

Farquhar, G. D., Caemmerer, S. V., and Berry, J. A.: A Biochemical-Model of Photosynthetic CO_2 Assimilation in Leaves of C_3 Species, Planta, 149, 78-90, doi:10.1007/BF00386231, 1980.

Goulden, M. L., Munger, J. W., Fan, S. M., Daube, B. C., and Wofsy, S. C.: Measurements of carbon sequestration by long-term eddy covariance: Methods and a critical evaluation of accuracy, Global Change Biol, 2, 169-182, doi:10.1111/j.1365-2486.1996.tb00070.x, 1996.

Hanson, P. J., Amthor, J. S., Wullschleger, S. D., Wilson, K., Grant, R. F., Hartley, A., Hui, D., Hunt, J., E Raymond, Johnson, D. W., and Kimball, J. S.: Oak forest carbon and water simulations: model intercomparisons and evaluations against independent data, Ecological Monographs, 74, 443-489, doi:10.1890/03-4049, 2004.

Helm, J., Hartmann, H., Göbel, M., Hilman, B., Herrera Ramírez, D., and Muhr, J.: Low-cost chamber design for simultaneous CO_2 and O_2 flux measurements between tree stems and the atmosphere, Tree Physiology, 41, 1767-1780, doi:10.1093/treephys/tpab022, 2021.

Hicks Pries, C., Angert, A., Castanha, C., Hilman, B., and Torn, M. S.: Using respiration quotients to track changing sources of soil respiration seasonally and with experimental warming, Biogeosciences, 17, 3045-3055, doi:10.5194/bg-17-3045-2020, 2020.

Hilman, B. and Angert, A.: Measuring the ratio of CO_2 efflux to O_2 influx in tree stem respiration, Tree Physiology, 36, 1422-1431, doi:10.1093/treephys/tpw057, 2016.

Hilman, B., Weiner, T., Haran, T., Masiello, C. A., Gao, X., and Angert, A.: The Apparent Respiratory Quotient of Soils and Tree Stems and the Processes That Control It, Journal of Geophysical Research: Biogeosciences, 127, e2021JG006676, doi:10.1029/2021JG006676, 2022.

Hilman, B., Muhr, J., Trumbore, S. E., Kunert, N., Carbone, M. S., Yuval, P., Wright, S. J., Moreno, G., Pérez-Priego, O., Migliavacca, M., Carrara, A., Grünzweig, J. M., Osem, Y., Weiner, T., and Angert, A.: Comparison of CO_2 and O_2 fluxes demonstrate retention of respired CO_2 in tree stems from a range of tree species, Biogeosciences, 16, 177-191, doi:10.5194/bg-16-177-2019, 2019.

Hockaday, W. C., Gallagher, M. E., Masiello, C. A., Baldock, J. A., Iversen, C. M., and Norby, R. J.: Forest soil carbon oxidation state and oxidative ratio responses to elevated CO_2, J Geophys Res-Biogeo, 120, 1797-1811, doi:10.1002/2015JG003010, 2015.

Ishidoya, S., Murayama, S., Kondo, H., Saigusa, N., Kishimoto-Mo, A. W., and Yamamoto, S.: Observation of O_2: CO_2 exchange ratio for net turbulent fluxes and its application to forest carbon cycles, Ecol Res, 30, 225-234, doi:10.1007/s11284-014-1241-3, 2015.

Ishidoya, S., Morimoto, S., Aoki, S., Taguchi, S., Goto, D., Murayama, S., and Nakazawa, T.: Oceanic and terrestrial biospheric CO2 uptake estimated from atmospheric potential oxygen observed at Ny-Alesund, Svalbard, and Syowa, Antarctica, Tellus B, 64, 2012.

Ishidoya, S., Sugawara, H., Terao, Y., Kaneyasu, N., Aoki, N., Tsuboi, K., and Kondo, H.: O_2 : CO_2 exchange ratio for net turbulent flux observed in an urban area of Tokyo, Japan, and its application to an evaluation of anthropogenic CO_2 emissions, Atmos Chem Phys, 20, 5293-5308, doi:10.5194/acp-20-5293-2020, 2020.

Ishidoya, S., Murayama, S., Takamura, C., Kondo, H., Saigusa, N., Goto, D., Morimoto, S., Aoki, N., Aoki, S., and Nakazawa, T.: O_2:CO_2 exchange ratios observed in a cool temperate deciduous forest ecosystem of central Japan, Tellus B, 65, doi:10.3402/tellusb.v65i0.21120, 2013.

Juergensen, J., Muhr, J., and Knohl, A.: Variations of the Oxidative Ratio across Ecosystem Components and Seasons in a Managed Temperate Beech Forest (Leinefelde, Germany), Forests, 12, 2021.

Keeling, R. F. and Manning, A. C.: 5.15 - Studies of Recent Changes in Atmospheric O_2 Content, in: Treatise on Geochemistry (Second Edition), edited by: Holland, H. D., and Turekian, K. K., Elsevier, Oxford, 385-404, doi:10.1016/B978-0-08-095975-7.00420-4, 2014.

Keeling, R. F. and Shertz, S. R.: Seasonal and interannual variations in atmospheric oxygen and implications for the global carbon cycle, Nature, 358, 723-727, doi:10.1038/358723a0, 1992.

Knohl, A. and Baldocchi, D. D.: Effects of diffuse radiation on canopy gas exchange processes in a forest ecosystem, J Geophys Res-Biogeo, 113, doi:10.1029/2007JG000663, 2008.

Knohl, A. and Buchmann, N.: Partitioning the net CO_2 flux of a deciduous forest into respiration and assimilation using stable carbon isotopes, Global Biogeochem Cy, 19, doi:10.1029/2004GB002301, 2005.

Lenschow, D. H., Mann, J., and Kristensen, L.: How Long Is Long Enough When Measuring Fluxes and Other Turbulence Statistics, J Atmos Ocean Tech, 11, 661-673, doi:10.1175/1520-0426(1994)011<0661:HLILEW>2.0.CO;2, 1994.

Manning, A. C. and Keeling, R. F.: Global oceanic and land biotic carbon sinks from the Scripps atmospheric oxygen flask sampling network, Tellus B, 58, 95-116, doi:10.1111/j.1600-0889.2006.00175.x, 2006.

Meredith, L., Commane, R., Munger, J., Dunn, A., Tang, J., Wofsy, S., and Prinn, R.: Ecosystem fluxes of hydrogen: a comparison of flux-gradient methods, Atmos Meas Tech, 7, 2787-2805, doi:10.5194/amt-7-2787-2014, 2014.

Ogee, J., Peylin, P., Cuntz, M., Bariac, T., Brunet, Y., Berbigier, P., Richard, P., and Ciais, P.: Partitioning net ecosystem carbon exchange into net assimilation and respiration with canopy-scale isotopic measurements: An error propagation analysis with $^{13}CO_2$ and $CO^{18}O$ data, Global Biogeochem Cy, 18, doi:10.1029/2003GB002166, 2004.

Oikawa, P. Y., Sturtevant, C., Knox, S. H., Verfaillie, J., Huang, Y. W., and Baldocchi, D. D.: Revisiting the partitioning of net ecosystem exchange of CO_2 into photosynthesis and respiration with simultaneous flux measurements of $^{13}CO_2$ and CO_2, soil respiration and a biophysical model, CANVEG, Agricultural and Forest Meteorology, 234-235, 149-163, doi:10.1016/j.agrformet.2016.12.016, 2017.

https://doi.org/10.5194/bg-2023-30
Preprint. Discussion started: 2 March 2023

Pickers, P. A., Manning, A. C., Sturges, W. T., Le Quéré, C., Mikaloff Fletcher, S. E., Wilson, P. A., and Etchells, A. J.: In situ measurements of atmospheric O_2 and CO_2 reveal an unexpected O_2 signal over the tropical Atlantic Ocean, Global Biogeochem Cy, 31, 1289-1305, doi:10.1002/2017GB005631, 2017.

Randerson, J., Masiello, C., Still, C., Rahn, T., Poorter, H., and Field, C.: Is carbon within the global terrestrial biosphere becoming more oxidized? Implications for trends in atmospheric O_2, Global Change Biol, 12, 260-271, doi:10.1111/j.1365-2486.2006.01099.x, 2006.

Raupach, M. R.: Applying Lagrangian fluid mechanics to infer scalar source distributions from concentration profiles in plant canopies, Agricultural and Forest Meteorology, 47, 85-108, doi:10.1016/0168-1923(89)90089-0, 1989.

Rebmann, C., Aubinet, M., Schmid, H., Arriga, N., Aurela, M., Burba, G., Clement, R., De Ligne, A., Fratini, G., Gielen, B., Grace, J., Graf, A., Gross, P., Haapanala, S., Herbst, M., Hortnagl, L., Ibrom, A., Joly, L., Kljun, N., Kolle, O., Kowalski, A., Lindroth, A., Loustau, D., Mammarella, I., Mauder, M., Merbold, L., Metzger, S., Molder, M., Montagnani, L., Papale, D., Pavelka, M., Peichl, M., Roland, M., Serrano-Ortiz, P., Siebicke, L., Steinbrecher, R., Tuovinen, J. P., Vesala, T., Wohlfahrt, G., and Franz, D.: ICOS eddy covariance flux-station site setup: a review, Int Agrophys, 32, 471-+, doi:10.1515/intag-2017-0044, 2018.

Schober, R.: Ausbauchungsreihen, Grundner, F., Schwappach, A, 1952.

Seibt, U., Brand, W. A., Heimann, M., Lloyd, J., Severinghaus, J. P., and Wingate, L.: Observations of O_2:CO_2 exchange ratios during ecosystem gas exchange, Global Biogeochem Cy, 18, doi:10.1029/2004GB002242, 2004.

Severinghaus, J.: Studies of the Terrestrial O2 and Carbon Cycles in Sand Dune Gases and in Biosphere 2, doi:10.2172/477735, 1995.

Stephens, B. B., Keeling, R. F., and Paplawsky, W. J.: Shipboard measurements of atmospheric oxygen using a vacuum-ultraviolet absorption technique, Tellus B: Chemical and Physical Meteorology, 55, 857-878, doi:10.3402/tellusb.v55i4.16386, 2003.

Tamrakar, R., Rayment, M. B., Moyano, F., Mund, M., and Knohl, A.: Implications of structural diversity for seasonal and annual carbon dioxide fluxes in two temperate deciduous forests, Agricultural and Forest Meteorology, 263, 465-476, doi:10.1016/j.agrformet.2018.08.027, 2018.

Tarantola, A.: Inverse Problem Theory and Methods for Model Parameter Estimation, Society for Industrial and Applied Mathematics, doi:10.1137/1.9780898717921, 2004.

Tcherkez, G., Nogues, S., Bleton, J., Cornic, G., Badeck, F., and Ghashghaie, J.: Metabolic origin of carbon isotope composition of leaf dark-respired CO_2 in French bean, Plant Physiol, 131, 237-244, doi:10.1104/pp.013078, 2003.

Tohjima, Y., Mukai, H., Machida, T., Hoshina, Y., and Nakaoka, S. I.: Global carbon budgets estimated from atmospheric O-2/N-2 and CO2 observations in the western Pacific region over a 15-year period, Atmos Chem Phys, 19, 9269-9285, 2019.

Van Oijen, M., Rougier, J., and Smith, R.: Bayesian calibration of process-based forest models: bridging the gap between models and data, Tree Physiology, 25, 915-927, doi:10.1093/treephys/25.7.915, 2005.

Wehr, R. and Saleska, S. R.: An improved isotopic method for partitioning net ecosystem-atmosphere CO_2 exchange, Agricultural and Forest Meteorology, 214, 515-531, doi:10.1016/j.agrformet.2015.09.009, 2015.

Wilson, J.: Turbulent transport within the plant canopy, 1989.

Worrall, F., Clay, G. D., Masiello, C. A., and Mynheer, G.: Estimating the oxidative ratio of the global terrestrial biosphere carbon, Biogeochemistry, 115, 23-32, doi:10.1007/s10533-013-9877-6, 2013.

Yakir, D. and Wang, X. F.: Fluxes of CO_2 and water between terrestrial vegetation and the atmosphere estimated from isotope measurements, Nature, 380, 515-517, doi:10.1038/380515a0, 1996.

Zobitz, J. M., Burns, S. P., Ogee, J., Reichstein, M., and Bowling, R.: Partitioning net ecosystem exchange of CO_2: A comparison of a Bayesian/isotope approach to environmental regression methods, J Geophys Res-Biogeo, 112, doi:10.1029/2006JG000282, 2007.